for the preparation of **37a**, the protected **37f** (34 mg, 0.025 mmol) was converted into 9.8 mg (10.5 μmol, 42%) of the title compound **37f**, as a freeze-dried powder.

$[\alpha]^{26}_D$ −32.0 (*c* 0.13, H_2O). t_R = 28.9 min (linear gradient of MeCN in H_2O, 10 to 40% over 30 min). *m/z* (ISMS): 714.0 (MH^+). Found (FAB-HRMS): 713.3903. Calcd for $C_{37}H_{49}O_5N_{10}$ (MH^+): 713.3887.

***(tert*-Butoxy)-*N*-[2(*R,S*)-hydroxy-1(*S*)-(2-naphthylmethyl)but-3-enyl]formamide, 20.** To a stirred solution of Boc-Nal-OMe **19** (4.0 g, 12.2 mmol) in CH_2Cl_2 (100 mL) was added dropwise a solution of DIBAL-H in toluene (1.0 M, 24.4 mL, 24.4 mmol) at −78 °C under argon, and the mixture was stirred at −78 °C for 2 h. To the solution was added dropwise a vinyl Grignard (CH_2=CHMgCl) reagent in THF (12.6 mL, 36.6 mmol) at −78 °C, and the mixture was stirred for 6 h with warming to 0 °C. The reaction was quenched with saturated aqueous citric acid at −78 °C, and organic solvents were concentrated under reduced pressure. The residue was extracted with EtOAc, and the extract was washed successively with saturated aqueous citric acid, saturated aqueous $NaHCO_3$, and brine and dried over $MgSO_4$. Concentration under reduced pressure followed by chromatography over silica gel with EtOAc/*n*-hexane (3:1) gave a mixture of *threo*- and *erythro*-allyl alcohols **20** (1.4 g, 35% yield from **19**) as a colorless oil. The mixture of diastereoisomer was used in the following step without further purification.

^{1}H NMR (270 MHz, $CDCl_3$) *δ*: 1.24−1.36 (9H, br, *tert*-Bu), 2.90−2.94 (1H, br, 2-H), 3.00−3.03 (2H, br, CH_2), 3.86−3.94 (1H, br, 1-H), 4.95−5.01 (1H, br, NH), 5.13−5.17 (1H, m, C*H*H=), 5.22−5.29 (1H, m, CH*H*=), 5.82−5.94 (1H, m, CH=), 7.38−7.43 (3H, m, ArH), 7.68−7.80 (4H, m, ArH). *m/z* (ISMS): 328.5 (MH^+). Found (FAB-HRMS): 328.1921. Calcd for $C_{20}H_{26}O_3N$ (MH^+): 328.1913.

1(*S*)-[1-[(*tert*-Butoxy)carbonylamino]-2-(naphthyl)ethyl]prop-2(*R, S*)-enyl Acetate, 21. To a stirred solution of allyl alcohol **20** (8.5 g, 26.0 mmol) in $CHCl_3$ (10 mL), were added acetic anhydride (11.0 mL, 117 mmol) and pyridine (18.9 mL, 234 mmol) at 4 °C, and the mixture was stirred at room temperature for 6 h. The mixture was concentrated under reduced pressure. The residue was extracted with EtOAc, and the extract was washed with aqueous 5% $NaHCO_3$, aqueous 1 M HCl, and brine and dried over $MgSO_4$. Concentration under reduced pressure followed by chromatography over silica gel with EtOAc/*n*-hexane (2:1) gave acetates **21** (5.7 g, 59% yield from **20**) as a colorless oil.

^{1}H NMR (270 MHz, $CDCl_3$) *δ*: 1.29−1.37 (9H, br, *tert*-Bu), 2.06−2.08 (3H, br, Me), 2.80−2.84 (1H, br, 2-H), 2.89−2.95 (2H, br, CH_2), 4.14−4.20 (1H, br, 1-H), 4.74−4.78 (1H, br, NH), 5.20−5.24 (1H, br m, C*H*H=), 5.25−5.30 (1H, br m, CH*H*=), 5.74−5.80 (1H, m, CH=), 7.30−7.42 (3H, m, ArH), 7.60−7.76 (4H, m, ArH). *m/z* (ISMS): 370.5 (MH^+). Found (FAB-HRMS): 370.2016. Calcd for $C_{22}H_{28}O_4N$ (MH^+): 370.2018.

***tert*-Butyl 4(*R,S*)-Acetoxy-5(*S*)-[(*tert*-butoxy)carbonylamino]-6-(2-naphthyl)hex-2-enoate, 22.** To a solution of acetate **21** (5.7 g, 15.4 mmol) in CH_2Cl_2 (40 mL) was bubbled O_3 gas at −78 °C until a blue color persisted. To the above solution, was added Me_2S (11 mL, 154 mmol), and the mixture was stirred for 30 min. The mixture was dried over $MgSO_4$. Concentration under reduced pressure gave an oily residue of a crude aldehyde, which was used immediately in the next step without further purification. To a stirred suspension of LiCl (1.57 g, 37 mmol) in MeCN (10 mL) under argon were added $(EtO)_2P(O)CH_2CO_2{}^tBu$ (8.7 mL, 37 mmol) and DIPEA (6.4 mL, 37 mmol) at 0 °C. After 20 min, the above aldehyde in MeCN (20 mL) was added to the above mixture at 0 °C, and the mixture was stirred at this temperature for 8 h. The mixture was concentrated under reduced pressure, and the residue was extracted with EtOAc. The extract was washed successively with saturated aqueous citric acid and H_2O and dried over $MgSO_4$. Concentration under reduced pressure followed by chromatography over silica gel with EtOAc/*n*-hexane (1:2) gave enoates **22** (2.1 g, 29% yield from **21**) as a white amorphous semisolid.

Found: C, 68.97; H, 7.60; N, 2.92. $C_{27}H_{35}O_6N$ Calcd: C, 69.06; H, 7.51; N, 2.98. ^{1}H NMR (270 MHz, $CDCl_3$) *δ*: 1.34−1.38 (9H, br, *tert*-Bu), 1.43−1.47 (9H, br, *tert*-Bu), 2.13−2.17 (3H, br, Me), 2.91−2.99 (2H, br, CH_2), 4.22−4.32 (1H, br, 5-H), 4.71−4.77 (1H, br, 4-H), 5.42−5.46 (1H, br, NH), 5.79−5.99 (1H, m, CH=), 6.70−6.83 (1H, m, CH=), 7.43−7.49 (3H, m, ArH), 7.77−7.82 (4H, m, Ar). *m/z* (FAB-LRMS): 468 [$(M-H)^-$], 305, 199, 153, 151, and 46 (base peak). Found (FAB-HRMS): 468.2375. Calcd for $C_{27}H_{34}O_6N$ [$(M-H)^-$]: 468.2386.

***tert*-Butyl 5(*S*)-[(*tert*-Butoxy)carbonylamino]-6-(2-naphthyl)hex-3-enoate (Boc-L-Nal=Gly-O^{t}Bu), 23.** To a stirred slurry of Sm (900 mg, 6.0 mmol) in dry THF (20 mL) under argon at room temperature was added a solution of CH_2I_2 (322 μL, 4.0 mmol) in dry THF (20 mL), and the slurry was stirred at room temperature for 2 h until a dark green color persisted. To a stirred solution of enoate **22** (600 mg, 1.3 mmol) in dry THF (16 mL) in the other vessel were added *tert*-BuOH (8 mL, excess) and the above SmI_2 solution (38 mL, 3.8 mmol) under argon at room temperature, and the mixture was stirred for 1 h. The reaction was then quenched with saturated aqueous NH_4Cl (10 mL) at 4 °C, and the mixture was extracted with Et_2O (20 mL). The extract was washed with saturated aqueous NH_4Cl and brine and dried over $MgSO_4$. Concentration under reduced pressure followed by chromatography over silica gel with EtOAc/*n*-hexane (1:4) gave the enoate **23** (530 mg, 95% yield from **22**) as white crystals.

Mp: 80−82 °C (from *n*-hexane). Found: C, 73.17; H, 8.17; N, 3.39. $C_{25}H_{33}O_4N$ Calcd: C, 72.96; H, 8.08; N, 3.40. $[\alpha]^{25}_D$ 11.00 (*c* 1.09, $CHCl_3$). ^{1}H NMR (400 MHz, $CDCl_3$) *δ*: 1.37 (9H, s, *tert*-Bu), 1.41 (9H, s, *tert*-Bu), 2.93 (2H, d, *J* = 6.4 Hz, 6-CH_2), 2.98 (2H, d, *J* = 6.8 Hz, 2-CH_2), 4.48−4.59 (1H, br, NH), 5.43 (1H, t, *J* = 11.2 Hz, 5-H), 5.55 (1H, dd, *J* = 15.6, 5.6 Hz, CH=), 5.61−5.69 (1H, br, CH=), 7.31−7.46 (3H, m, ArH), 7.60−7.62 (1H, br, ArH), 7.74−7.78 (3H, m, ArH). *m/z* (ISMS): 412.0 (MH^+). Found (FAB-HRMS): 412.2491. Calcd for $C_{25}H_{34}O_4N$ (MH^+): 412.5418.

5(*S*)-[(Fluoren-9-ylmethoxy)carbonylamino]-6-(2-naphthyl)hex-3-enoic Acid (Fmoc-L-Nal=Gly-OH), 24. The enoate **23** (1.79 g, 4.35 mmol) was dissolved in TFA (30 mL), anisole (472 μL, 4.35 mmol) was added to the solution at 4 °C, and the mixture was stirred at room temperature for 2 h. The mixture was concentrated under reduced pressure and dissolved in THF and H_2O (1:1 (v/v) 20 mL). To the stirred solution were added Fmoc-OSu (1.47 g, 4.35 mmol) and Et_3N (10 mL, 71.7 mmol) at 4 °C, and the mixture was stirred at room temperature for 8 h. The mixture was acidified with aqueous 1 M HCl and was extracted with EtOAc. The extract was washed with aqueous 0.1 M HCl and brine and dried over $MgSO_4$. Concentration under reduced pressure followed by chromatography over silica gel with EtOAc/*n*-hexane (3:1) gave the enoic acid **24** (1.61 g, 78% yield from **23**) as white crystals.

Mp: 134−136 °C (from *n*-hexane). $[\alpha]^{23}_D$ −2.75 (*c* 0.73, $CHCl_3$). ^{1}H NMR (400 MHz, $CDCl_3$) *δ*: 2.96 (2H, br, 6-CH_2), 3.03 (2H, br, 2-CH_2), 4.14 (1H, t, *J* = 6.6 Hz, ArH), 4.32 (1H, dd, *J* = 14.9, 7.2 Hz, CH=), 4.38 (1H, m, CH=) 4.54 (1H, d, *J* = 7.6 Hz, CH_2), 4.81 (1H, br, 5-H), 5.62 (1H, br, NH), 7.18−7.28 (2H, m, ArH), 7.30−7.52 (5H, m, ArH), 7.57−7.63 (2H, m, ArH), 7.70−7.79 (6H, m, ArH). *m/z* (ISMS): 478.0 (MH^+). Found (FAB-HRMS): 478.2016. Calcd for $C_{31}H_{28}O_4N$ (MH^+): 478.2018.

H-D-Tyr(O^{t}Bu)-Arg(Pbf)-Arg(Pbf)-Nal-ψ[(*E*)-CH=CH]-Gly-NHNHCO−Wang Resin. On the hydrazide resin, were coupled successively Fmoc-D-Tyr(O^{t}Bu)-OH, Fmoc-Nal-ψ[(*E*)-CH=CH]-Gly-OH, and Fmoc-Arg(Pbf)-OH by use of the procedure identical with that described for the preparation of H-D-Tyr(O^{t}Bu)-Arg(Pbf)-Arg(Mts)-ψ[(*E*)-CH=CH]-Nal-Gly-NHNHCO−Wang resin to afford the protected **37c** resin.

***cyclo*(-D-Tyr-Arg-Arg-Nal-ψ[(*E*)-CH=CH]-Gly-)·2TFA (37c).** By use of a procedure identical with that described for the preparation of **37a**, the protected **37c** resin (173 mg, 0.13 mmol) was converted into 7.0 mg (7.4 μmol, 5.9%) of the title compound **37c**, as a freeze-dried powder.

$[\alpha]^{21}_D$ −43.1 (*c* 0.33, H_2O). t_R = 24.3 min (linear gradient of MeCN in H_2O, 10 to 40% over 30 min). *m/z* (ISMS): 713.0

(MH$^+$). Found (FAB-HRMS): 713.3911. Calcd for $C_{37}H_{49}O_5N_{10}$ (MH$^+$): 713.3887.

***tert*-Butyl 2(*S*)-[[2(*S*)-[(*tert*-butoxy)carbonyamino]-5-[[imino[(2,4,6-trimethylphenyl)sulfonyl]amino]methyl]-amino]pentyl]amino]-3-(2-naphthyl) Propanoate [Boc-L-Arg(Mts)-ψ[CH$_2$–NH]-L-Nal-O^{t}Bu], 26.** To a stirred solution of **25** (5.0 g, 10 mmol) in toluene/CH_2Cl_2 (1:1 (v/v), 50 mL) was added dropwise a solution of DIBAL-H in toluene (1.0 M, 60 mL, 60 mmol) at −50 °C under argon, and the mixture was stirred for 4 h at −78 °C. The reaction was quenched with saturated aqueous citric acid at −78 °C, and the organic solvents were concentrated under reduced pressure. The residue was extracted with EtOAc, and the extract was washed successively with saturated aqueous citric acid and brine and dried over $MgSO_4$. Concentration under reduced pressure gave a crude aldehyde (Boc-Arg(Mts)-H), which was used in the following step without further purification. To the stirred solution of Boc-Arg(Mts)-H in $ClCH_2CH_2Cl$/DMF (1:6 (v/v), 100 mL), were added H-L-Nal-O^{t}Bu (5.4 g, 20 mmol) and AcOH (1.1 mL, 20 mmol) at 4 °C and stirred for 10 min. $NaBH(OAc)_3$ (6.4 g, 30 mmol) was added to the above mixture at 4 °C and stirred for 8 h with warming to room temperature. The mixture was concentrated under reduced pressure, and the residue was extracted with $CHCl_3$. The extract was washed with aqueous 5% $NaHCO_3$ and brine and dried over $MgSO_4$. Concentration under reduced pressure gave an oily residue, which was purified by chromatography over silica gel with $CHCl_3$/MeOH (39:1) to yield 3.4 g (4.9 mmol, 49% yield from **25**) of compound **26** as a yellow oil.

$[\alpha]^{23}_D$ 4.08 (*c* 1.96, $CHCl_3$). ^{1}H NMR (270 MHz, $CDCl_3$) δ: 1.24 (9H, s, *tert*-Bu), 1.32 (9H, s, *tert*-Bu), 1.55 (2H, br m, 4-CH$_2$), 1.74 (2H, br m, 3-CH$_2$), 2.25 (3H, s, Ar-*p*-Me), 2.67 (6H, s, Ar-*o*-Me), 3.08 (2H, br m, 5-CH$_2$), 3.20 (2H, br, 3-CH$_2$), 3.34 (2H, br, 1-CH$_2$), 3.62 (1H, br, 2-H), 3.82 (1H, br, 2-H), 3.99 (1H, br, NH), 5.95 (1H, br, NH), 6.61 (3H, br, guanidino), 6.87 (2H, s, Ar-*m*-H), 7.36–7.44 (3H, m, ArH), 7.67–7.75 (4H, m, ArH). *m/z* (ISMS): 697.0 (MH$^+$). Found (FAB-HRMS): 696.3812. Calcd for $C_{37}H_{54}O_6N_5S$ (MH$^+$): 696.3795.

***tert*-Butyl 2(*S*)-[*N*-[2(*S*)-[(*tert*-Butoxy)carbonylamino]-5-[[imino[(2,4,6-trimethylphenyl)sulfonyl]amino]methyl]-amino]pentyl](phenylmethoxy)carbonylamino]-3-(2-naphthyl)propanoate [Boc-Arg(Mts)-ψ[CH$_2$–N(Cbz)]-Nal-O^{t}Bu], 27.** To a stirred solution of propanoate **26** (1.4 g, 2.0 mmol) in DMF (100 mL) at 4 °C, were added Cbz-Cl (0.69 g, 4.0 mmol) and Et_3N (560 μL, 4.0 mmol) and stirred at room temperature for 8 h. The mixture was concentrated under reduced pressure and extracted with EtOAc. The extract was washed with saturated aqueous citric acid, saturated aqueous $NaHCO_3$, and brine and dried over $MgSO_4$. Concentration under reduced pressure followed by chromatography over silica gel with EtOAc/*n*-hexane (1:1) gave the title compound **27** (1.6 g, 77% yield from **26**) as a yellow oil.

$[\alpha]^{23}_D$ −36.44 (*c* 0.67, $CHCl_3$). ^{1}H NMR (270 MHz, $CDCl_3$) δ: 1.39 (9H, s, *tert*-Bu), 1.42 (9H, s, *tert*-Bu), 1.47 (2H, s, 4-CH$_2$), 1.64 (2H, br, 3-CH$_2$), 2.42 (3H, s, Ar-*p*-Me), 2.65 (6H, s, Ar-*o*-Me), 2.98 (2H, br, 5-CH$_2$), 3.27 (2H, br, 3-CH$_2$), 3.31 (2H, br, 1-CH$_2$), 3.40 (1H, br, 2-H), 4.24 (1H, br, 2-H), 5.08 (2H, s, CH$_2$), 5.90 (1H, br, NH), 6.13 (3H, br, guanidino), 6.86 (2H, s, Ar-*m*-H), 7.26 (5H, s, ArH), 7.31–7.46 (3H, m, ArH), 7.54–7.75 (4H, m, ArH). *m/z* (ISMS): 831.5 (MH$^+$). Found (FAB-HRMS): 830.4153. Calcd for $C_{45}H_{60}O_8N_5S$ (MH$^+$): 830.4163.

2(*S*)-[*N*-[2(*S*)-[(Fluoren-9-ylmethoxy)carbonylamino]-5-[[imino[(2,4,6-trimethylphenyl)sulfonyl]amino]methyl]-amino]pentyl](phenylmethoxy)carbonylamino]-3-(2-naphthyl)propanoic Acid [Fmoc-Arg(Mts)-ψ[CH$_2$–N(Cbz)]-Nal-OH], 28. The propanoate **27** (1.3 g, 1.57 mmol) was dissolved in TFA (30 mL), anisole (170 μL, 1.57 mmol) was added to the solution at 4 °C, and the mixture was stirred at room temperature for 2 h. The mixture was concentrated under reduced pressure and dissolved in THF and H_2O (1:1 (v/v) 100 mL). To the stirred solution were added Fmoc-OSu (530 mg, 1.57 mmol) and Et_3N (10 mL, 71.7 mmol) at 4 °C, and the mixture was stirred at room temperature for 8 h. The mixture was acidified with aqueous 1 M HCl and extracted with EtOAc. The extract was washed with aqueous 0.1 M HCl and brine and dried over $MgSO_4$. Concentration under reduced pressure followed by chromatography over silica gel with EtOAc/*n*-hexane (4:1) gave the propanoic acid **28** (1.39 g, 99% yield from **27**) as white crystals.

Mp: 156–158 °C (from *n*-hexane). $[\alpha]^{24}_D$ −8.17 (*c* 1.96, $CHCl_3$). ^{1}H NMR (270 MHz, $CDCl_3$) δ: 1.85 (2H, br, 4-CH$_2$), 1.93 (2H, br, 3-CH$_2$), 2.11 (3H, s, Ar-*p*-Me), 2.47 (6H, s, Ar-*o*-Me), 3.03 (2H, br, 5-CH$_2$), 3.22 (2H, br, 3-H), 3.37 (2H, br, 1-CH$_2$), 4.08 (1H, br, ArH), 4.15 (2H, br, CH$_2$), 4.30 (1H, br, 2-H), 5.16 (1H, br, NH), 6.36 (3H, br, guanidino), 6.83 (2H, s, Ar-*m*-H) 7.25 (5H, s, ArH), 7.29–7.40 (6H, m, ArH), 7.50–7.83 (9H, m, ArH). *m/z* (ISMS): 897.0 (MH$^+$). Found (FAB-HRMS): 896.3693. Calcd for $C_{51}H_{54}O_8N_5S$ (MH$^+$): 896.3710.

H-D-Tyr(O^{t}Bu)-Arg(Pbf)-Arg(Mts)-ψ[CH$_2$–NH]-Nal-Gly-NHNHCO–Wang Resin. On the hydrazide resin were coupled successively Fmoc-Gly-OH, Fmoc-Arg-ψ[CH$_2$–N(Cbz)]-Nal-OH, Fmoc-Arg(Pbf)-OH, and Fmoc-D-Tyr(O^{t}Bu)-OH by use of a procedure identical with that described for the preparation of H-D-Tyr(O^{t}Bu)-Arg(Pbf)-Arg(Mts)-ψ[(*E*)-CH=CH]-Nal-Gly-NHNHCO–Wang resin to afford the protected **37b** resin.

***cyclo*(-D-Tyr-Arg-Arg-ψ[CH$_2$–NH]-Nal-Gly-)·3TFA (37b).** By use of a procedure identical with that described for the preparation of **37a**, the protected **37b** (200 mg, 0.15 mmol) was converted into 0.6 mg (0.57 μmol, 0.86%) of the title compound **37b**, as a freeze-dried powder.

$[\alpha]^{21}_D$ −22.6 (*c* 0.27, H_2O). t_R = 19.3 min (linear gradient of MeCN in H_2O, 10 to 40% over 30 min). *m/z* (ISMS): 717.0 (MH$^+$). Found (FAB-HRMS): 716.4016. Calcd for $C_{36}H_{49}O_5N_{11}$ (MH$^+$): 716.3996.

***tert*-Butyl 2(*S*)-[[2-[(*tert*-Butoxy)carbonylamino]-3-(2-naphthyl)propyl]amino]acetate [Boc-L-Nal-ψ[CH$_2$–NH]-Gly-O^{t}Bu], 30.** To a stirred solution of Boc-Nal-NMe(OMe) **29** (5.5 g, 15 mmol) in toluene/CH_2Cl_2 (1:1 (v/v) 50 mL) was added dropwise a solution of DIBAL-H in toluene (1.0 M, 62 mL, 62 mmol) at −78 °C under argon, and the mixture was stirred at −78 °C for 4 h. The reaction was quenched with saturated aqueous citric acid at −78 °C, and organic solvents were concentrated under reduced pressure. The residue was extracted with EtOAc, and the extract was washed successively with saturated aqueous citric acid and brine and dried over $MgSO_4$. Concentration under reduced pressure gave a crude aldehyde (Boc-Nal-H), which was used in the following step without further purification. To the stirred solution of Boc-Nal-H in $ClCH_2CH_2Cl$/DMF (1:6 (v/v), 200 mL), was added H-Gly-O^{t}Bu·AcOH (5.8 g, 31 mmol) at 4 °C and stirred for 10 min. $NaBH(OAc)_3$ (9.8 g, 46 mmol) was added to the above mixture at 4 °C and stirred for 8 h with warming to room temperature. The mixture was concentrated under reduced pressure, and the residue was extracted with $CHCl_3$. The extract was washed with aqueous 5% $NaHCO_3$ and brine and dried over $MgSO_4$. Concentration under reduced pressure gave an oily residue, which was purified by chromatography over silica gel with $CHCl_3$ to yield 3.2 g (7.7 mmol, 50% yield from **29**) of compound **30** as a yellow oil.

$[\alpha]^{22}_D$ −0.67 (*c* 4.47, $CHCl_3$). ^{1}H NMR (400 MHz, $CDCl_3$) δ: 1.38 (9H, s, *tert*-Bu), 1.47 (9H, s, *tert*-Bu), 2.87 (2H, br, CH$_2$), 3.02 (2H, br, 3-CH$_2$), 3.85–3.94 (2H, m, 1-CH$_2$), 4.09–4.21 (1H, m, 2-H), 5.44 (1H, br, NH), 6.45 (1H, br, NH), 7.29–7.36 (2H, m, Ar–H), 7.41–7.48 (2H, m, ArH), 7.60–7.62 (1H, m, ArH), 7.72–7.83 (2H, m, ArH). *m/z* (ISMS): 415.5 (MH$^+$). Found (FAB-HRMS): 415.2594. Calcd for $C_{24}H_{35}O_4N_2$ (MH$^+$): 415.2597.

***tert*-Butyl 2(*S*)-[*N*-[2-[(*tert*-Butoxy)carbonylamino]-3-(2-naphthyl)propyl](phenylmethoxy)carbonylamino]acetate [Boc-L-Nal-ψ[CH$_2$–N(Cbz)]-Gly-O^{t}Bu], 31.** To a stirred solution of acetate **30** (5.0 g, 12.1 mmol) in DMF (100 mL) at 4 °C were added Cbz-Cl (20.6 g, 121 mmol) and DIPEA (21.7 mL, 121 mmol), and the mixture was stirred at room temperature for 8 h. The mixture was concentrated under reduced pressure and extracted with EtOAc. The solution was washed with saturated aqueous citric acid, saturated aqueous $NaHCO_3$, and brine and dried over $MgSO_4$. Concentration under

reduced pressure followed by chromatography over silica gel with EtOAc/*n*-hexane (1:2) gave the title compound **31** (4.0 g, 60% yield from **30**) as white crystals.

Mp: 107−109 °C (from *n*-hexane). Found: C, 70.01; H, 7.42 N, 4.98. Calcd for $C_{32}H_{40}O_6N_2$: C, 70.05; H, 7.35; N, 5.11. $[\alpha]^{23}_D$ −14.73 (*c* 0.48, $CHCl_3$). ^1H NMR (400 MHz, $CDCl_3$) δ: 1.34 (9H, s, *tert*-Bu), 1.35 (9H, s, *tert*-Bu), 2.94 (2H, br, CH_2), 3.37 (2H, br, 3-CH_2), 3.88 (2H, m, 1-CH_2), 4.05 (1H, m, 2-H), 4.94 (1H, br, NH), 5.13 (2H, s, CH_2), 7.28−7.33 (5H, br, ArH), 7.35−7.47 (3H, m, ArH), 7.74−7.81 (4H, m, ArH). *m/z* (ISMS): 549.5 (MH^+). Found (FAB-HRMS): 549.2953. Calcd for $C_{32}H_{41}O_6N_2$ (MH^+): 549.2965.

2(*S*)-[*N*-[2-[(Fluoren-9-ylmethoxy)carbonylamino]-3-(2-naphthyl)propyl](phenylmethoxy)carbonylamino]-acetic Acid [Fmoc-L-Nal-ψ[CH_2−N(Cbz)]-Gly-OH], 32. The acetate **31** (4.0 g, 7.29 mmol) was dissolved in TFA (30 mL), anisole (792 μL, 7.29 mmol) was added to the solution at 4 °C, and the mixture was stirred at room temperature for 2 h. The mixture was concentrated under reduced pressure and dissolved in THF and H_2O (1:1 (v/v) 100 mL). To the stirred solution, were added Fmoc-OSu (2.46 g, 7.29 mmol) and Et_3N (10 mL, 71.7 mmol) at 4 °C, and the mixture was stirred at room temperature for 8 h. The mixture was acidified with aqueous 1 M HCl and was extracted with EtOAc. The extract was washed with aqueous 0.1 M HCl and brine and dried over $MgSO_4$. Concentration under reduced pressure followed by chromatography over silica gel with $CHCl_3$/MeOH (39:1) gave the title compound **32** (4.20 g, 94% yield from **31**) as a yellow oil.

$[\alpha]^{23}_D$ −5.01 (*c* 4.79, $CHCl_3$). ^1H NMR (400 MHz, $CDCl_3$) δ: 2.99 (2H, d, J = 6.4 Hz, 3-CH_2), 3.41 (2H, s, CH_2), 4.00 (2H, br, 1-CH_2), 4.08 (1H, t, J = 6.6 Hz, Ar−H), 4.24 (1H, t, J = 6.2 Hz, 2-H), 4.27 (2H, br, CH_2), 5.05 (2H, s, CH_2), 5.53 (1H, d, J = 8.0 Hz, NH), 7.18 (5H, s, Ar−H) 7.30−7.50 (8H, m, ArH), 7.61−7.73 (7H, m, ArH). *m/z* (ISMS): 615.0 (MH^+). Found (FAB-HRMS): 615.2509. Calcd for $C_{38}H_{35}O_6N_2$ (MH^+): 615.2495.

H-D-Tyr(O^{t}Bu)-Arg(Pbf)-Arg(Pbf)-Nal-ψ[CH_2−N(Cbz)]-Gly-NHNHCO−Wang Resin. On the hydrazide resin, were coupled successively Fmoc-D-Tyr(O^{t}Bu)-OH, Fmoc-Nal-ψ[CH_2−N(Cbz)]-Gly-OH, and Fmoc-Arg(Pbf)-OH by use of a procedure identical with that described for the preparation of H-D-Tyr-(O^{t}Bu)-Arg(Pbf)-Arg(Mts)-ψ[(*E*)-CH=CH]-Nal-Gly-NHNHCO−Wang resin to afford the protected **37d** resin.

***cyclo*(-D-Tyr-Arg-Arg-Nal-ψ[CH_2−NH]-Gly-)·3TFA (37d).** By use of a procedure identical with that described for the preparation of **37a**, the protected **37d** (173 mg, 0.13 mmol) was converted into 7.0 mg (7.4 μmol, 5.9%) of the title compound **37d**, as a freeze-dried powder.

$[\alpha]^{19}_D$ −58.0 (*c* 0.69, H_2O). t_R = 21.0 min (linear gradient of MeCN in H_2O, 10 to 40% over 30 min). *m/z* (ISMS): 717.0 (MH^+). Found (FAB-HRMS): 716.4003. Calcd for $C_{36}H_{49}O_5N_{11}$ (MH^+): 716.3996.

Cell Culture. Human T-cell lines, MT-4, and MOLT-4 cells were grown in RPMI 1640 medium containing 10% heat-inactivated fetal calf serum, 100 IU/mL penicillin, and 100 μg/mL streptomycin.

Virus. A strain of X4-HIV-1, HIV-1$_{IIIB}$, was used for the anti-HIV assay. This virus was obtained from the culture supernatant of HIV-1 persistently infected MOLT-4/HIV-1$_{IIIB}$ cells and stored at −80 °C until used.

Anti-HIV-1 Assay. Anti-HIV-1 activity was determined based on the protection against HIV-1-induced cytopathogenicity in MT-4 cells. Various concentrations of test compounds were added to HIV-1-infected MT-4 cells at a multiplicity of infection (MOI) of 0.01 and placed in wells of a flat-bottomed microtiter tray (1.5 × 10^4 cells/well). After 5 days incubation at 37 °C in a CO_2 incubator, the number of viable cells was determined using the 3-(4,5-dimethylthiazol-2-yl)-2,5-diphenyltetrazolium bromide (MTT) method (EC_{50}).[48] Cytotoxicity of compounds was determined based on the viability of mock-infected cells using the MTT method (CC_{50}). 3′-Azido-3′-dideoxythymidine (AZT) was tested as a control.

[^{125}I]-SDF-1 Binding and Displacement. Stable CHO cell transfectants expressing CXCR4 variants were prepared as described previously.[49] CHO transfectants were harvested by treatment with trypsin/EDTA, allowed to recover in complete growth medium (MEM-α, 100 μg/mL penicillin, 100 μg/mL streptomycin, 0.25 μg/mL amphotericin B, 10% (v/v)) for 4−5 h, and then washed in cold binding buffer (PBS containing 2 mg/mL BSA). For ligand binding, the cells were resuspended in binding buffer at 1 × 10^7 cells/mL, and 100 μL aliquots were incubated with 0.1 nM of [^{125}I]-SDF-1 (PerkinElmer Life Sciences) for 2 h on ice under constant agitation. Free and bound radioactivities were separated by centrifugation of the cells through an oil cushion, and bound radioactivity was measured with a gamma counter (Cobra, Packard, Downers Grove, IL). Inhibitory activity of FC131 analogues was determined based on the inhibition of [^{125}I]-SDF-1-binding to CXCR4 transfectants (IC_{50}).

NMR Spectroscopy (37a and 37c). The peptide sample was dissolved in DMSO-d_6 at a concentration of 5 mM. ^1H NMR spectra of the peptides were recorded at 300 K. The assignments of the proton resonances were achieved by use of ^1H−^1H COSY spectra. $^3J(H^N, H^\alpha)$ coupling constants were measured from one-dimensional spectra. The mixing time for the nuclear Overhauser spectroscopy (NOESY) experiments was set at 400 ms. NOESY spectra were composed of 512 real points in the F2 dimension and 256 real points, which were zero-filled to 256 points in the F1 dimension, with 144 scans per t1 increment. The cross-peak intensities were evaluated by relative buildup rates of the cross peaks. Temperature dependence of the chemical shifts of all of the amide bonds was investigated in **37a** and **37c**. The only temperature coefficient for the NH of Arg^5 was small, but NOE was not observed between the D-Tyr^3 C$^\alpha$H and the Arg^5 NH in both **37a** and **37c**. Thus, no hydrogen bond restraints were used in the simulated annealing calculations.

Calculation of Structures. The structure calculations were performed on a Silicon Graphics Origin 2000 workstation with the NMR refine program within the Insight II/Discover package using the consistent valence force field (CVFF).[51] Pseudoatoms were defined for the methylene protons of Nal^1, D-Tyr^3, Arg^4, and Arg^5, prochiralities of which were not identified by ^1H NMR data. The restraints, in which the Gly^2 α-methylene participated, were defined for the separate protons without definition of the prochiralities. The dihedral ϕ angle constraints were calculated based on the Karplus equation: $^3J(H^N,H^\alpha) = 6.7\cos^2(\theta - 60°) - 1.3\cos(\theta - 60°) + 1.5$.[52] Lower and upper angle errors were set to 15°. The NOESY spectrum with a mixing time of 400 ms was used for the estimation of the distance restraints between protons. The NOE intensities were classified into three categories (strong, medium, and weak) based on the number of contour lines in the cross peaks to define the upper-limit distance restraints (2.7, 3.5, and 5.0 Å, respectively). The upper-limit restraints were increased by 1.0 Å for the involved pseudoatoms. Lower bounds between nonbonded atoms were set to their van der Waals radii (1.8 Å). These distance and dihedral angle restraints were included with force constants of 25−100 kcal/mol·Å^2 and 25−100 kcal/mol·rad^2, respectively. The 50 initial structures generated by the NMR refine program randomly were subjected to the simulated annealing calculations. The final minimization stage was achieved until the maximum derivative became less than 0.01 kcal/mol·Å^2 by the steepest descents and conjugate gradients methods.

Acknowledgment. This work was supported in part by a 21st Century COE Program "Knowledge Information Infrastructure for Genome Science", a Grant-in-Aid for Scientific Research from the Ministry of Education, Culture, Sports, Science and Technology, Japan and the Japan Health Science Foundation. Computation time was provided by the Supercomputer Laboratory, Institute for Chemical Research, Kyoto University. S.U. is

grateful for a Research Fellowship from the Japan Society for the Promotion of Science for Young Scientists.

Supporting Information Available: HPLC charts for synthetic compounds of **37a**, **37b**, **37c**, **37d**, and **37f**. These materials are available free of charge via the Internet at http://pubs.acs.org.

References

(1) Kaltenbronn, J. S.; Hudspeth, J. P.; Lunney, E. A.; Michniewicz, B. M.; Nicolaides, E. D.; Repine, J. T.; Roark, W. H.; Stier, M. A.; Tinney, F. J.; Woo, P. K. W.; Essenburg, A. D. Renin inhibitors containing isosteric replacements of the amide bond connecting the P_3 and P_2 sites. *J. Med. Chem.* **1990**, *33*, 838–845.

(2) Ibuka, T.; Habashita, H.; Otaka, A.; Fujii, N. A highly stereoselective synthesis of (*E*)-alkene dipeptide isosteres via organocyanocopper–lewis acid mediated reaction. *J. Org. Chem.* **1991**, *56*, 4370–4382.

(3) Wipf, P.; Fritch, P. C. S_N2' reactions of peptide aziridines. A cuprate-based approach to (*E*)-alkene isosteres. *J. Org. Chem.* **1994**, *59*, 4875–4886.

(4) Fujii, N.; Nakai, K.; Tamamura, H.; Otaka, A.; Mimura, N.; Miwa, Y.; Taga, T.; Yamamoto, Y.; Ibuka, T. S_N2' ring opening of aziridines bearing an α,β-unsaturated ester group with organocopper reagents. A new stereoselective synthetic route to (*E*)-alkene dipeptide isosteres. *J. Chem. Soc., Perkin Trans. 1* **1995**, 1359–1371.

(5) Daly, M. J.; Ward, R. A.; Thompson, D. F.; Procter, G. Allylsilanes in organic synthesis; stereoselective synthesis of *trans*-alkene peptide isosteres. *Tetrahedron Lett.* **1995**, *36*, 7545–7548.

(6) Tamamura, H.; Hiramatsu, K.; Miyamoto, K.; Omagari, A.; Oishi, S.; Nakashima, H.; Yamamoto, N.; Kuroda, Y.; Nakagawa, T.; Otaka, A.; Fujii, N. Synthesis and evaluation of pseudopeptide analogues of a specific CXCR4 inhibitor, T140: The insertion of an (*E*)-alkene dipeptide isostere into the βII′-turn moiety. *Bioorg. Med. Chem. Lett.* **2002**, *12*, 923–928.

(7) Tamamura, H.; Koh, Y.; Ueda, S.; Sasaki, Y.; Yamasaki, T.; Aoki, M.; Maeda, K.; Watai, Y.; Arikuni, H.; Otaka, A.; Mitsuya, H.; Fujii, N. Reduction of peptide character of HIV protease inhibitors that exhibit nanomolar potency against multi-drug resistant HIV-1 strains. *J. Med. Chem.* **2003**, *46*, 1764–1768.

(8) Tamamura, H.; Yamashita, M.; Muramatsu, H.; Ohno, H.; Ibuka, T.; Otaka, A.; Fujii, N. Regiospecific ring-opening reactions of aziridines bearing an α,β-unsaturated ester group with trifluoroacetic acid or methanesulfonic acid: Application to the stereoselective synthesis of (*E*)-alkene dipeptide isosteres. *Chem. Commun.* **1997**, 2327–2328.

(9) Tamamura, H.; Yamashita, M.; Nakajima, Y.; Sakano, K.; Otaka, A.; Ohno, H.; Ibuka, T.; Fujii, N. Regiospecific ring-opening reactions of β-aziridinyl α,β-enoates with acids: application to the stereoselective synthesis of a couple of diastereoisomeric (*E*)-alkene dipeptide isosteres from a single β-aziridinyl α,β-enoate and to the convenient preparation of amino alcohols bearing α,β-unsaturated ester groups. *J. Chem. Soc., Perkin Trans. 1*, **1999**, 2983–2996.

(10) Oishi, S.; Tamamura, H.; Yamashita, M.; Odagaki, Y.; Hamanaka, N.; Otaka, A.; Fujii, N. Stereoselective synthesis of a set of two functionalized (*E*)-alkene dipeptide isosteres of L-amino acid-L-Glu and L-amino acid-D-Glu. *J. Chem. Soc., Perkin Trans. 1* **2001**, 2445–2451.

(11) Nakamura, E.; Aoki, S.; Sekiya, K.; Oshino, H.; Kuwajima, I. Carbon–carbon bond-forming reactions of zinc homoenolate of esters. A novel three-carbon nucleophile with general synthetic utility. *J. Am. Chem. Soc.* **1987**, *109*, 8056–8066.

(12) Ochiai, H.; Tamaru, Y.; Tsubaki, K.; Yoshida, Z. Unsaturated ester synthesis via copper(I)-catalyzed allylation of zinc esters. *J. Org. Chem.* **1987**, *52*, 4418–4420.

(13) Yeh, M. C. P.; Knochel, P. 2-Cyanoethylzinc iodide: A new reagent with reactivity umpolung.*Tetrahedron Lett.* **1988**, *29*, 2395–2396.

(14) Knochel, P.; Yeh, M. C. P.; Berk, S. C.; Talbert, J. Synthesis and reactivity toward acyl chlorides and enones of the new highly functionalized copper reagents RCu(CN)ZnI. *J. Org. Chem.* **1988**, *53*, 2390–2392.

(15) Zhu, L.; Wehmeyer, R. M.; Rieke, R. D. The direct formation of functionalized alkyl(aryl)zinc halides by oxidative addition of highly reactive zinc with organic halides and their reactions with acid chlorides, α,β-unsaturated ketones, and allylic, aryl, and vinyl halides. *J. Org. Chem.* **1991**, *56*, 1445–1453.

(16) Fujii, N.; Oishi, S.; Hiramatsu, K.; Araki, T.; Ueda, S.; Tamamura, H.; Otaka, A.; Kusano, S.; Terakubo, S.; Nakashima, H.; Broach, J. A.; Trent, J. O.; Wang, Z.; Peiper, S. C. Molecular-size reduction of a potent CXCR4–chemokine antagonist using orthogonal combination of conformation- and sequence-based libraries. *Angew. Chem., Int. Ed.* **2003**, *42*, 3251–3253.

(17) Koshiba, T.; Hosotani, R.; Miyamoto, Y.; Ida, J.; Tsuji, S.; Nakajima, S.; Kawaguchi, M.; Kobayashi, H.; Doi, R.; Hori, T.; Fujii, N.; Imamura, M. Expression of stromal cell-derived factor 1 and CXCR4 ligand receptor system in pancreatic cancer: a possible role for tumor progression. *Clin. Cancer. Res.* 2000, *6*, 3530–3535.

(18) Müller, A.; Homey, B.; Soto, H.; Ge, N.; Catron, D.; Buchanan, M. E.; McClanahan, T.; Murphy, E.; Yuan, W.; Wagner, S. N.; Barrera, J. L.; Mohar, A.; Verastegui, E.; Zlotnik, A. Involvement of chemokine receptors in breast cancer metastasis. *Nature* **2001**, *410*, 50–56.

(19) Tamamura, H.; Hori, A.; Kanzaki, N.; Hiramatsu, K.; Mizumoto, M.; Nakashima, H.; Yamamoto, N.; Otaka, A.; Fujii, N. T140 analogs as CXCR4 antagonists identified as anti-metastatic agents in the treatment of breast cancer. *FEBS Lett.* **2003**, *550*, 79–83.

(20) Feng, Y.; Broder, C. C.; Kennedy, P. E.; Berger, E. A. HIV-1 entry co-factor: Functional cDNA cloning of a seven-transmembrane, G protein-coupled receptor. *Science* **1996**, *272*, 872–877.

(21) Nanki, T.; Hayashida, K.; EI–Gabalawy, H. S.; Suson, S.; Shi, K.; Girschick, H. J.; Yavuz, S.; Lipsky, P. E. Stromal cell-derived factor-1-CXC chemokine receptor interactions play a central role in CD4$^+$ T cell accumulation in rheumatoid arthritis synovium. *J. Immunol.* **2000**, *165*, 6590–6598.

(22) Tamamura, H.; Fujisawa, M.; Hiramatsu, K.; Mizumoto, M.; Nakashima, H.; Yamamoto, N.; Otaka, A.; Fujii, N. Identification of a CXCR4 antagonist, a T140 analog, as an anti-rheumatoid arthritis agent. *FEBS Lett.* **2004**, *569*, 99–104.

(23) Murakami, T.; Nakajima, T.; Koyanagi, Y.; Tachibana, K.; Fujii, N.; Tamamura, H.; Yoshida, N.; Waki, M.; Matsumoto, A.; Yoshie, O.; Kishimoto, T.; Yamamoto, N.; Nagasawa, T. A small molecule CXCR4 inhibitor that blocks T cell line-tropic HIV-1 infection. *J. Exp. Med.*, **1997**, *186*, 1389–1393.

(24) Schols, D.; Struyf, S.; Van Damme, J.; Este, J. A.; Henson, G.; De Clercq, E. Inhibition of T-tropic HIV strains by selective antagonization of the chemokine receptor CXCR4. *J. Exp. Med.* **1997**, *186*, 1383–1388.

(25) Donzella, G. A.; Schols, D.; Lin, S. W.; Este J. A.; Nagashima, K. A.; Maddon, P. J.; Allaway, G. P.; Sakmar, T. P.; Henson, G.; De Clercq, E.; Moore, J. P. AMD3100, a small molecule inhibitor of HIV-1 entry via the CXCR4 co-receptor. *Nat. Med.* **1998**, *4*, 72–77.

(26) Doranz, B. J.; Grovit-Ferbas, K.; Sharron, M. P.; Mao, S.-H.; Bidwell Goetz, M.; Daar, E. S.; Doms, R. W.; O'Brien, W. A. A small-molecule inhibitor directed against the chemokine receptor CXCR4 prevents its use as an HIV-1 coreceptor. *J. Exp. Med.* **1997**, *186*, 1395–1400.

(27) Howard, O. M. Z.; Oppenheim, J. J.; Hollingshead, M. G.; Covey, J. M.; Bigelow, J.; McCormack, J. J.; Buckheit, Jr., R. W.; Clanton, D. J.; Turpin, J. A.; Rice, W. G. Inhibition of in vitro and in vivo HIV replication by a distamycin analogue that interferes with chemokine receptor function: a candidate for chemotherapeutic and microbicidal application. *J. Med. Chem.* **1998**, *41*, 2184–2193.

(28) Tamamura, H.; Xu, Y.; Hattori, T.; Zhang, X.; Arakaki, R.; Kanbara, K.; Omagari, A.; Otaka, A.; Ibuka, T.; Yamamoto, N.; Nakashima, H.; Fujii, N. A low molecular weight inhibitor against the chemokine receptor CXCR4: a strong anti-HIV peptide T140. *Biochem. Biophys. Res. Commun.* **1998**, *253*, 877–882.

(29) Tamamura, H.; Omagari, A.; Oishi, S.; Kanamoto, T.; Yamamoto, N.; Peiper, S. C.; Nakashima, H.; Otaka, A.; Fujii, N. Pharmacophore identification of a specific CXCR4 inhibitor, T140, leads to development of effective anti-HIV agents with very high selectivity indexes. *Bioorg. Med. Chem. Lett.* **2000**, *10*, 2633–2637.

(30) Fujii, N.; Nakashima, H.; Tamamura, H. The therapeutic potential of CXCR4 antagonists in the treatment of HIV. *Expert Opin. Invest. Drugs* **2003**, *12*, 185–195.

(31) Fukami, T.; Nagase, T.; Fujita, K.; Hayama, T.; Niiyama, K.; Mase, T.; Nakajima, S.; Fukuroda, T.; Saeki, T.; Nishikibe, M.; Ihara, M.; Yano, M.; Ishikawa, K. Structure–activity relationships of cyclic pentapeptide endothelin A receptor antagonists. *J. Med. Chem.* **1995**, *38*, 4309–4324.

(32) Haubner, R.; Gratias, R.; Diefenbach, B.; Goodman, S. L.; Jonczyk, A.; Kessler, H. Structural and functional aspects of RGD-containing cyclic pentapeptides as highly potent and selective integrin $\alpha V\beta 3$ antagonists. *J. Am. Chem. Soc.* **1996**, *118*, 7461–7472.

(33) Spatola, A. F.; Crozet, Y.; deWit, D.; Yanagisawa, M. Rediscovering an endothelin antagonist (BQ-123): A self-deconvoluting cyclic pentapeptide library. *J. Med. Chem.* **1996**, *39*, 3842−3846.
(34) Wermuth, J.; Goodman, S. L.; Jonczyk, A.; Kessler, H. Stereoisomerism and biological activity of the selective and superactive αVβ3 integrin inhibitor cyclo(−RGDfV-) and its retro-inverso peptide. *J. Am. Chem. Soc.* **1997**, *119*, 1328−1335.
(35) Haubner, R.; Finsinger, D.; Kessler, H. Stereoisomeric peptide libraries and peptidomimetics for designing selective inhibitors of the αVβ3 integrin for a new cancer therapy. *Angew. Chem., Int. Ed. Engl.* **1997**, *36*, 1374−1389.
(36) Porcelli, M.; Casu, M.; Lai, A.; Saba, G.; Pinori, M.; Cappelletti, S.; Mascagni, P. Cyclic pentapeptides of chiral sequence DLDDL as scaffold for antagonism of G-protein coupled receptors: Synthesis, activity and conformational analysis by NMR and molecular dynamics of ITF 1565 a substance P inhibitor. *Biopolymers* **1999**, *50*, 211−219.
(37) Oishi, S.; Kamano, T.; Niida, A.; Odagaki, Y.; Hamanaka, N.; Yamamoto, M.; Ajito, K.; Tamamura, H.: Otaka, A.; Fujii, N. Diastereoselective synthesis of new ψ[[(*E*)-CH=CMe]- and ψ[[(*Z*)-CH=CMe]-type alkene dipeptide isosteres by organocopper reagents and application to conformationally restricted cyclic RGD peptidomimetics. *J. Org. Chem.* **2002**, *67*, 6162−6173.
(38) Tamamura, H.; Hiramatsu, K.; Kusano, S.; Terakubo, S.; Yamamoto, N.; Trent, J. O.; Wang, Z.; Peiper, S. C.; Nakashima, H.; Otaka, A.; Fujii, N. Synthesis of potent CXCR4 inhibitors possessing low cytotoxicity and improved biostability based on T140 derivatives. *Org. Biomol. Chem.* **2003**, *1*, 3656−3662.
(39) Tamamura, H.; Hiramatsu, K.; Mizumoto, M.; Ueda, S.; Kusano, S.; Terakubo, S.; Akamatsu, M.; Yamamoto, N.; Trent, J. O.; Wang, Z.; Peiper, S. C.; Nakashima, H.; Otaka, A.; Fujii, N. Enhancement of the T140-based pharmacophores leads to the development of more potent and bio-stable CXCR4 antagonists. *Org. Biomol. Chem.* **2003**, *1*, 3663−3669.
(40) Inagawa, J.; Ishikawa, M.; Yamaguchi, M. A mild and convenient method for the reduction of organic halides by using a SmI_2-THF solution in the presence of hexamethylphosphoric triamide (HMPA). *Chem. Lett.* **1987**, 1485−1486.
(41) Otaka, A.; Yukimasa, A.; Watanabe, J.; Sasaki, Y.; Oishi, S.; Tamamura, H.; Fujii, N. Application of samarium diiodide (SmI_2)-induced reduction of γ-acetoxy-α,β-enoates with α-specific kinetic electrophilic trapping for the synthesis of amino acid derivatives. *Chem. Commun.* **2003**, 1834−1835.
(42) Fukuyama, T.; Jow, C. K.; Cheng, M. 2- and 4-nitrobenzenesulfonamides: exceptionally versatile means for preparation of secondary amines and protection of amines. *Tetrahedron Lett.* **1995**, *36*, 6373−6374.
(43) Maligres, P. E.; See, M. M.; Askin, D.; Reider, P. J. Nosylaziridines: activated aziridine electrophiles. *Tetrahedron Lett.* **1997**, *38*, 5253−5256.
(44) Mitsunobu, O. The use of diethyl azodicarboxylate and triphenylphosphine in synthesis and transformation of natural products. *Synthesis* **1981**, *1*, 1−28.
(45) Blanchette, M. A.; Choy, W.; Davis, J. T.; Essenfeld, A. P.; Masamune, S.; Roush, R. W.; Sakai, T. Horner-Wadsworth-Emmons reaction: Use of lithium chloride and an amine for base-sensitive compounds. *Tetrahedron Lett.* **1984**, *25*, 2183−2186.
(46) Abdel-Magid, A. F.; Maryanoff, C. A.; Carson, K. G. Reductive amination of aldehydes and ketones by using sodium triacetoxyborohydride. *Tetrahedron Lett.* **1990**, *31*, 5595−5598.
(47) Honzl, J.; Rudinger, J. Amino acids and peptides. XXXIII. Nitrosyl chloride and butyl nitrite as reagents in peptide synthesis by the azide method; suppression of amide formation. *Collect. Czech. Chem. Commun.* **1961**, *26*, 2333−2344.
(48) Nakashima, H.; Masuda, M.; Murakami, T.; Koyanagi, Y.; Matsumoto, A.; Fujii, N.; Yamamoto, N. Anti-human immunodeficiency virus activity of a novel synthetic peptide, T22 ([Tyr-5, 12, Lys-7]polyphemusin II): a possible inhibitor of virus-cell fusion. *Antimicrob. Agents Chemother.* **1992**, *36*, 1249−1255.
(49) Navenot, J. M.; Wang, Z. X.; Trent, J. O.; Murray, J. L.; Hu, Q. X.; DeLeeuw, L.; Moore, P. S.; Chang, Y.; Peiper, S. C. Molecular anatomy of CCR5 engagement by physiologic and viral chemokines and HIV-1 envelope glycoproteins: Differences in primary structural requirements for RANTES, MIP-1α, and vMIP-II binding. *J. Mol. Biol.* **2001**, *313*, 1181−1193.
(50) Intramolecular hydrogen bonds were not observed in the calculated structure. Thus, the EADI-containing pseudopeptides, which are discussed in this study, do not seem to exist in a characteristic turn conformation such as a βII′γ turn as reported in several papers concerning normal cyclic pentapeptides, see Nikiforovich, G. V.; Kover, K. E.; Zhang, W.-J.; Marshall, G. R. Cyclopentapeptides as flexible conformational templates. *J. Am. Chem. Soc.* **2000**, *122*, 3262−3273.
(51) Miyamoto, K.; Nakagawa, T.; Kuroda, Y. Solution structure of the cytoplasmic linker between domain III−S6 and domain IV−S1 (III−IV linker) of the rat brain sodium channel in SDS micelles. *Biopolymers* **2001**, *59*, 380−393.
(52) Ludvigsen, S.; Andersen, K. V.; Poulsen, F. M. Accurate measurements of coupling-constants from 2-dimensional nuclear-magnetic-resonance spectra of proteins and determination of φ-angles *J. Mol. Biol.* **1991**, *217*, 731−736.

JM049429H

Identification of Novel Low Molecular Weight CXCR4 Antagonists by Structural Tuning of Cyclic Tetrapeptide Scaffolds

Hirokazu Tamamura,*,⊥,# Takanobu Araki,⊥ Satoshi Ueda,⊥ Zixuan Wang,§ Shinya Oishi,⊥ Ai Esaka,⊥ John O. Trent,∥ Hideki Nakashima,† Naoki Yamamoto,‡ Stephen C. Peiper,§ Akira Otaka,⊥ and Nobutaka Fujii*,⊥

Graduate School of Pharmaceutical Sciences, Kyoto University, Sakyo-ku, Kyoto 606-8501, Japan; Institute of Biomaterials and Bioengineering, Tokyo Medical and Dental University, Chiyoda-ku Tokyo 101-0062, Japan; Medical College of Georgia, Augusta, Georgia 30912; James Graham Brown Cancer Center, University of Louisville, Louisville, Kentucky 40202; St. Marianna University, School of Medicine, Miyamae-ku, Kawasaki 216-8511, Japan; and Tokyo Medical and Dental University, School of Medicine, Bunkyo-ku, Tokyo 113-8519, Japan

Received January 5, 2005

A highly potent CXCR4 antagonist, compound **2**, was previously found by using two orthogonal cyclic pentapeptide libraries involving conformation-based and sequence-based libraries based on the pharmacophore of a 14-mer peptidic antagonist, **1**. Herein, cyclic tetrapeptides derived from replacements of the dipeptide unit (Nal-Gly) with a γ-amino acid and pseudopeptides cyclized by disulfide and olefin bridges were synthesized to find novel scaffold structures different from that of cyclic pentapeptides. These compounds contain a reduced number of peptide bonds compared to compound **2**. Furthermore, several analogues with chemical modification of the side chain of Arg^4 in **2** were also prepared. From these, several new leads possessing high to moderate CXCR4-antagonistic activity were characterized.

Introduction

The chemokine receptor, CXCR4, is a seven transmembrane (7TM) GPCR that transduces signals of its endogenous ligand, stromal cell-derived factor-1 (SDF-1).[1−4] The SDF-1/CXCR4 system plays an important role in the migration of progenitors during embryologic development of the cardiovascular, hemopoietic, and central nervous systems. Recently, this system has been shown to be involved in several diseases, including HIV infection,[5] cancer metastasis/progression,[6−20] and rheumatoid arthritis (RA).[21] CXCR4 was initially identified as a coreceptor that is utilized in T cell line-tropic (X4-) HIV-1 entry.[5] Müller et al. reported that CXCR4 and another chemokine receptor, CCR7, are highly expressed in human breast cancer cells, while SDF-1 and a CCR7 ligand, CCL21, are highly expressed in lymph nodes, bone marrow, lung, and liver, which represent the primary metastatic destinations of breast cancer, suggesting that the SDF-1/CXCR4 system might determine the metastatic destination of tumor cells.[6] Recently, this system has been recognized to be involved in the metastasis of several types of cancers, such as pancreatic cancer,[7,8] melanoma,[6,9] prostate cancer,[10] kidney cancer,[11] neuroblastoma,[12] non-Hodgkin's lymphoma,[13] lung cancer,[14] ovarian cancer,[15,16] multiple myeloma,[17] chronic lymphocytic leukemia,[18] acute lymphoblastic leukemia,[19] and malignant brain tumor.[20] Nanki et al. reported that the memory T cells highly express CXCR4 and the SDF-1 concentration is extremely high in the synovium of RA patients, and that

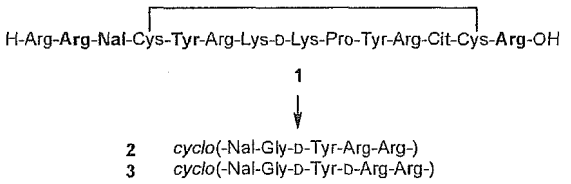

Figure 1. Reduction of the molecular size of a peptide **1** to cyclic pentapeptides **2** and **3**. Bold residues are the indispensable residues of **1** for the expression of strong CXCR4-antagonistic activity.

SDF-1 stimulates migration of the memory T cells and inhibits T cell apoptosis, indicating that the SDF−CXCR4 interaction plays a critical role in T cell accumulation in the RA synovium.[21] Thus, CXCR4 is thought to be an important therapeutic target for these diseases. Compound **1** and its analogues, 14-mer peptides, were previously found to be specific CXCR4 antagonists that were characterized as HIV-entry inhibitors,[22] anticancer-metastatic agents[8,23] and anti-RA agents.[24] Arg^2, L-3-(2-naphthyl)alanine $(Nal)^3$, Tyr^5, and Arg^{14} were proven to constitute the critical pharmacophores of **1** (Figure 1).[25] The efficient utilization of two orthogonal cyclic pentapeptide libraries consisting of conformation-based and sequence-based libraries involving the critical residues of **1** led to molecular-size reduction of **1** and discovery of cyclic pentapeptides, **2** and **3**, which have strong CXCR4-antagonistic activity, comparable to that of **1**.[26] In this paper, we describe the fine-tuning of ring structures based on cyclic pentapeptide templates,[27−34] and chemical modifications of side chains for an increase in potency and a reduction of the peptide characteristics of **2**.[35]

Chemistry

γ-Amino Acid-Containing Cyclic Tetrapeptides (11a−d). Requisite N^{γ}-Fmoc-γ-amino acids, (2*E*,4*S*)-N^{γ}-

* Corresponding authors. Tel: +81 75 753 4551, Fax: +81 75 753 4570, e-mail: tamamura@pharm.kyoto-u.ac.jp and nfujii@pharm.kyoto-u.ac.jp.
⊥ Kyoto University.
Institute of Biomaterials and Bioengineering.
§ Medical College of Georgia.
∥ University of Louisville.
† St. Marianna University.
‡ School of Medicine.

10.1021/jm050009h CCC: $30.25
Published on Web 04/13/2005

Scheme 1[a]

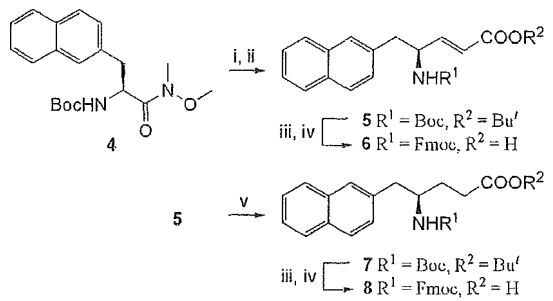

[a] Reagents: (i) DIBAL-H; (ii) $(EtO)_2P(O)CH_2CO_2Bu^t$,LiCl, DIPEA; (iii) 95% aqueous TFA; (iv) Fmoc-OSu, Et_3N; (v) H_2, Pd/C.

Scheme 2[a]

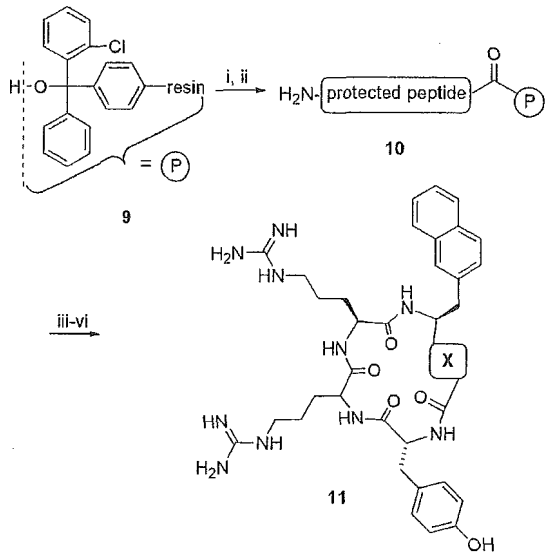

Compd.	Sequence (*cyclo*)	X
11a	(-γ-Nal[1]-D-Tyr[2]-D-Arg[3]-Arg[4]-)	$-CH_2-CH_2-$
11b	(-γ-Nal[1]-D-Tyr[2]-Arg[3]-Arg[4]-)	$-CH_2-CH_2-$
11c	(-γ-(*E*)-Nal[1]-D-Tyr[2]-D-Arg[3]-Arg[4]-)	-CH=CH-
11d	(-γ-(*E*)-Nal[1]-D-Tyr[2]-Arg[3]-Arg[4]-)	-CH=CH-

[a] Reagents: (i) **6** or **8**, DIPEA, DMF/CH_2Cl_2; (ii) Fmoc-based SPPS; (iii) $AcOH/TFE/CH_2Cl_2$; (iv) DPPA, $NaHCO_3$; (v) basic alumina column; (vi) 95% aqueous TFA.

Fmoc-4-amino-5-naphthalen-2-yl-pent-2-enoic acid (γ-(*E*)-Nal) **6** and (4*R*)-*N*γ-Fmoc-4-amino-5-naphthalen-2-yl-pentanoic acid (γ-Nal) **8**, were synthesized according to Scheme 1. Boc-Nal-NMe(OMe) **4** was treated with DIBAL followed by modified Horner–Wadsworth–Emmons olefination to yield Boc-γ-(*E*)-Nal-OBu^t **5**. N^{α}-Fmoc-protection after the cleavage of the N^{α}-Boc and Bu^t groups of **5** with TFA afforded a desired compound, Fmoc-γ-(*E*)-Nal-OH **6**. Hydrogenation of **5** obtained a reduced compound, **7**, which was similarly converted to another desired compound, Fmoc-γ-Nal-OH **8**. The protected peptide resin **10** was constructed by general Fmoc-based solid-phase synthesis on a (2-chloro)trityl resin **9**, in which the above γ-amino acid, **6** or **8**, was introduced as a C-terminal residue by DIPEA in DMF/CH_2Cl_2 (Scheme 2). Cleavage of the liner peptide from the resin with $AcOH/TFE/CH_2Cl_2$ (1:1:3 (v/v)) followed by cyclization with diphenylphosphoryl azide (DPPA) and $NaHCO_3$, subsequent deprotection with TFA and HPLC purification gave the desired cyclic peptide **11**.[26]

Scheme 3[a]

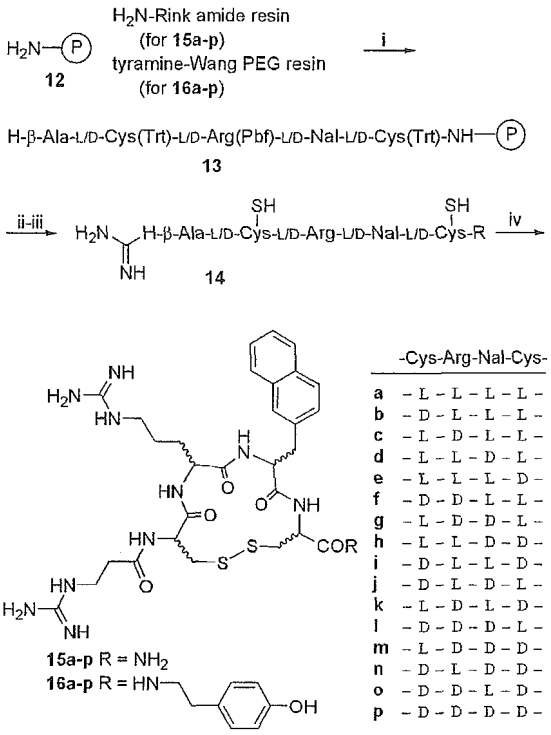

	-Cys-Arg-Nal-Cys-
a	- L - L - L - L -
b	- D - L - L - L -
c	- L - D - L - L -
d	- L - L - D - L -
e	- L - L - L - D -
f	- D - D - L - L -
g	- L - D - D - L -
h	- L - L - D - D -
i	- D - L - L - D -
j	- D - L - D - L -
k	- L - D - L - D -
l	- D - D - D - L -
m	- L - D - D - D -
n	- D - L - D - D -
o	- D - D - L - D -
p	- D - D - D - D -

[a] Reagents: (i) Fmoc-based SPPS; (ii) 1*H*-pyrazole-1-carboxamidine hydrochloride, DIPEA; (iii) $EDT/H_2O/TFA$; (iv) aqueous $AcONH_4$ pH 8.

Disulfide-Bridged Cyclic Peptides (15a–p and 16a–p). The protected peptide resin was constructed by general Fmoc-based solid-phase synthesis on an NH_2-Rink amide resin (for **15a–p**) or a tyramine-Wang PEG resin (for **16a–p**) **12** (Scheme 3). Fmoc-β-Ala-OH was condensed to the N-terminus of the protected resin as the final residue. After deprotection of the Fmoc group, N-guanylation of the resulting free β-amino group with 1*H*-pyrazole-1-carboxamidine hydrochloride and DIPEA, followed by cleavage from the resin and removal of the 2,2,4,6,7-pentamethyldihydrobenzofuran-5-sulfonyl (Pbf) and Trt groups with $EDT/H_2O/TFA$, gave the crude reduced peptide (2SH-peptide) **14**. Subsequent air-oxidation of the crude 2SH-peptide **14** and HPLC purification yielded the desired disulfide peptide **15** or **16**.

Disulfide-Bridged Cyclic Peptides (15q and 16q). The protected peptide resin was constructed on an Fmoc-NH-Rink amide resin (for **15q**) or an Fmoc-tyramine-Wang PEG resin (for **16q**) in the same manner as in the synthesis of **15e** or **16e** (Table 1). Reductive amination of the N-terminal amino group of the protected resin with *N*-Fmoc-3-aminopropanal and $NaBH(OAc)_3$,[36] followed by removal of the Fmoc group and the subsequent N-guanylation of the resulting free amino group in the same manner as in the synthesis of **15e** or **16e**, obtained the protected pseudo-peptide resin. Cleavage from the resin and removal of the Pbf and Trt groups, the subsequent air-oxidation, and HPLC purification were performed in the same manner as in the

Table 1. Inhibitory Activity of Disulfide/Olefin-Bridged Cyclic Peptides against SDF-1 Binding to CXCR4

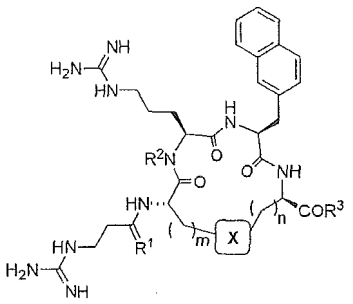

compd	m	n	X	R^1	R^2	R^3	$IC_{50} \pm SD$ (μM)[a]
15e	1	1	S–S	O	H	NH_2	0.69 ± 0.40
16e	1	1	S–S	O	H	tyramine	0.53 ± 0.28
15q	1	1	S–S	H_2	H	NH_2	ca. 1
16q	1	1	S–S	H_2	H	tyramine	ca. 1
15r	1	1	S–S	O	Me	NH_2	>10
16r	1	1	S–S	O	Me	tyramine	>10
20a	1	1	(*E*)-CH=CH	O	H	NH_2	1–10
20b	1	2	(*E*)-CH=CH	O	H	NH_2	1–10
20c	2	2	(*E*)-CH=CH	O	H	NH_2	1–10
20d	1	1	(*E*)-CH=CH	O	H	tyramine	1–10
2							0.0043 ± 0.0012
3							0.0084 ± 0.0038

[a] IC_{50} values are based on the inhibition of [^{125}I]-SDF-1 binding to CXCR4 transfectants of CHO cells. All data with standard deviation (SD) are the mean values for at least three independent experiments.

synthesis of **15e** or **16e** to yield the desired pseudopeptide, **15q** or **16q**.

Disulfide-bridged Cyclic Peptides (15r and 16r). The protected peptide resin was constructed on an Fmoc-NH-Rink amide resin (for **15r**) or an Fmoc-tyramine-Wang PEG resin (for **16r**) (Table 1). N^{α}-Methylation of the Arg(Pbf) residue in the protected resin was performed by the Fukuyama–Mitsunobu reaction.[37] N^{α}-*o*-Nitrobenzenesulfonyl (Ns) protection of H-Arg(Pbf)-Nal-D-Cys-NH-Rink amide (or -tyramine-Wang PEG) resin and the subsequent N^{α}-methylation with MeOH, Ph_3P, and diethyl azodicarboxylate (DEAD) were followed by removal of the N^{α}-Ns group with DBU and 2-mercaptoethanol. The next residue Fmoc-D-Tyr(Bu^t)-OH was condensed to the secondary N^{α}-amino group of the MeArg(Pbf) residue on the protected resin by using HATU, HOAt, and DIPEA. N-Guanylation, cleavage, deprotection, air-oxidation, and HPLC purification were subjected to yield the desired peptide, **15r** or **16r**.

Olefin-Bridged Cyclic Peptides (20a–d). The protected peptide resin was constructed on an NH_2-Rink amide resin (for **20a–c**) or an Fmoc-tyramine-Wang PEG resin (for **20d**) (Scheme 4) **12**. D-2-Allylglycine[38] (for **20a** or **20d**) or Fmoc-D-2-homoallylglycine[39,40] (for **20b** or **20c**) was used as the C-terminal residue, while Fmoc-L-2-allylglycine[41] (for **20a**, **20b**, or **20d**) or Fmoc-L-2-homoallylglycine[42] (for **20c**) was used as the N-terminal second residue. Fmoc-β-Ala-OH was condensed to the N-terminus of the protected resin as the final residue. The protected peptide resin **17** was subjected to ring-closing olefin metathesis with Grubbs catalyst second generation[43] to give the cyclized peptide resin **18**. After deprotection of the Fmoc group, N-guanylation of the resulting free β-amino group, followed by treatment with 1 M TMSBr-thioanisole/TFA and HPLC purification, gave the desired peptide **20**. The *E* geometry of the olefin units in **20a–d** was easily established from the coupling constants (J = 15.5, 15.6, 15.2, and 15.2 Hz, respectively) of the two olefinic protons by ^{1}H NMR analysis.

Scheme 4[a]

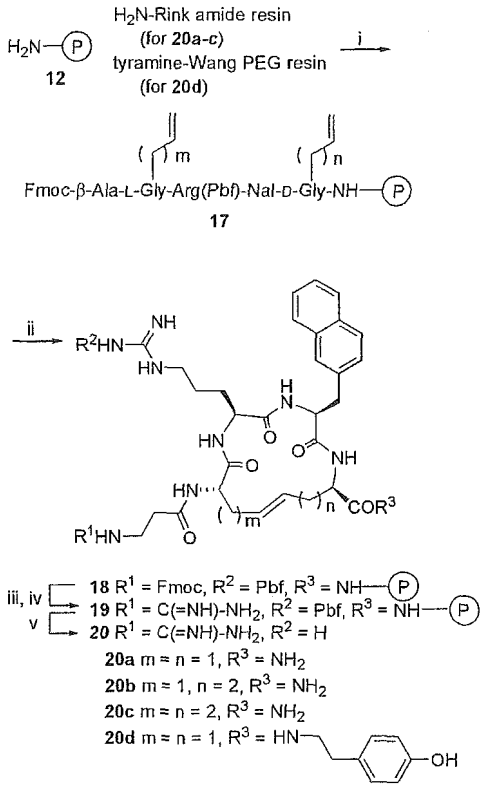

[a] Reagents: (i) Fmoc-based SPPS; (ii) Grubbs catalyst 2nd generation, (iii) piperdine; (iv) 1*H*-pyrazole-1-carboxamidine hydrochloride, DIPEA; (v) 1 M TMSBr-thioanisole/TFA.

Analogues with Substitution for Arg^4 (23a–p). Each peptide was synthesized in a general manner similar to that in the synthesis of **11a**, **23d** and **23f**: N^{α}-Methylation and coupling reaction to the N^{α}-methylated residue were performed in a manner similar to that in the synthesis of **15r**, **23j,k** and **23o,p**: After cyclization and deprotection, N-guanylation of the resulting free γ- or ϵ-amino group of the L-2,4-diaminobutyric acid (Dab)^4 or Lys^4 residue (for **23j** or **23k**, respectively) was performed with 1*H*-pyrazole-1-carboxamidine hydrochloride and DIPEA (Scheme 5). N-Guanylation of the resulting free γ-amino group of the *trans*- or *cis*-4-aminoproline residue[44] (for **23o** or **23p**, respectively) was similarly performed.

Biological Results and Discussion

γ-Amino Acid-Containing Cyclic Tetrapeptides. Cyclic pentapeptides, **2** and **3**, have a Gly residue as a spacer for cyclization. To reduce the ring size, the Nal-Gly sequences of **2** and **3** were replaced by a γ-Nal or γ-(*E*)-Nal unit (Scheme 2). Among these γ-amino acid-containing cyclic tetrapeptides (**11a–d**), only **11a** [substitution of γ-Nal for Nal-Gly of **3**] showed high CXCR4-antagonistic activity (IC_{50} = 54 nM) (Figure 2), although

Scheme 5[a]

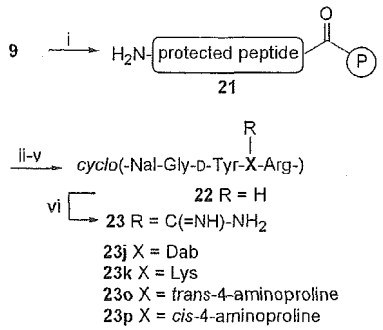

[a] Reagents: (i) Fmoc-based SPPS; (ii) AcOH/TFE/CH_2Cl_2 (1:1:3 (v/v)); (iii) DPPA, $NaHCO_3$; (iv) basic alumina column; (v) 95% aqueous TFA; (vi) 1*H*-pyrazole-1-carboxamidine hydrochloride, DIPEA.

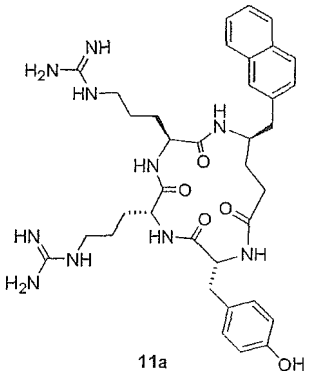

11a
IC_{50} = 54 ± 18 nM

Figure 2. The structure of **11a**.

this activity is 6-fold lower than that of **3**. This result suggested that the Gly residue and the amide bond of the Nal-Gly sequence are not necessary for high activity. The reason for no significant activity of **11b** [substitution of γ-Nal for Nal-Gly of **2**] (IC_{50} > 1 μM) cannot be well explained, however, the difference of chirality of L/D-Arg^3 in **2** and **3** might cause a global conformational change of the ring. Both γ-(*E*)-Nal-substituted analogues, **11c** and **11d**, showed no significant activity (IC_{50} > 1 μM), suggesting that constraint of the γ-amino acid to the *E*-form might not be suitable.

Disulfide-Bridged Cyclic Peptides. To optimize the ring structures of compound **2**-derived compounds, the use of scaffold templates different from that of cyclic pentapeptides was investigated. Since the four requisite residues of **1** are disposed in close vicinity each other due to the disulfide bridge [Cys^4-Cys^{13}][45] and cyclic peptides possessing the Arg-Arg-Nal sequence, such as **2** and **3**, showed high CXCR4-antagonistic activity, we designed and separately prepared disulfide-bridged cyclic peptide libraries consisting of the *N*-3-guanidinopropanoyl-L/D-Cys(S-)-L/D-Arg-L/D-Nal-L/D-Cys-(S-)-NH_2 (or −tyramine) sequence, which included 32 compounds (2 × 2^4 stereoisomers) (**15a−p** or **16a−p**, respectively, Scheme 3). Among these synthetic compounds, **15e** [*N*-3-guanidinopropanoyl-Cys(S-)-Arg-Nal-D-Cys(S-)-NH_2] and **16e** [*N*-3-guanidinopropanoyl-Cys-(S-)-Arg-Nal-D-Cys(S-)-tyramine] exhibited moderate CXCR4-antagonistic activity (IC_{50} = 690 and 530 nM, respectively) (Table 1), although the other compounds did not show any activity up to the concentration of 1 μM. **15e** and **16e** have a common combination of chiralities of composed amino acids, suggesting that these compounds form similar conformations. It seems that a phenol group of **16e** is not disposed in the suitable position, since **15e** and **16e** have almost the same potencies. However, notably, L,L-chiralities of Arg-Nal are critical for high activity, as shown in **2** and **3**. The synthetic Arg side chain involving an *N*-3-guanidinopropanoyl moiety has an extra atom, compared to the original Arg side chain. This might account for the lower activity.

In addition, **15e/16e** analogues, **15q** and **16q**, in which the amide bond of *N*-3-guanidinopropanoyl-Cys was replaced by a reduced amide bond, and **15r** and **16r**, in which the α-amino group of Arg was N-methylated, were prepared. Substitution of the reduced amide bond for the amide bond of *N*-3-guanidinopropanoyl-Cys brought about no significant difference in potency (IC_{50} of **15q** and **16q** = c.a. 1 μM). This suggested that the planar character of this amide bond and the carbonyl group have little effect on potency. N-Methylation of Arg caused remarkable decrease in potency (IC_{50} of **15r** and **16r** > 10 μM), indicating that conformation surrounded by the Cys-Arg amide bond might be changed or the Cys-Arg amide proton might be required for high activity.

Olefin-Bridged Cyclic Peptides. Cyclic analogues that were bridged by an olefin instead of a disulfide in **15e** and **16e** were synthesized. C-Terminal-amidated compounds, **20a-c**, which differ in bridge length, and a C-terminal tyramide-type compound, **20d**, showed lower activity (IC_{50} = 1−10 μM), compared to those of **15e** and **16e** (Table 1). It is thought that the constraint of the olefin unit into the *E*-form is not an effective optimization component.

Analogues Constrained in the Peripheral Region of Arg^4. The significant difference of activity between **23e** ([Ala^4]-**2**, Ala-substitution for Arg^4, IC_{50} = 63 nM) and **23c** ([D-Ala^4]-**2** = [D-Ala^4]-**3**, D-Ala-substitution for L/D-Arg^4, IC_{50} = 230 nM) indicates a biological importance of the amide bond direction between D-Tyr and L/D-Arg. Thus, relationships between the conformation surrounded by Arg^4 of **2** and activity were investigated. L/D-Pro-substitutions for Arg^4 also gave the difference of activity: An L-Pro-substituted analogue, **23b**, is 4-fold stronger than a D-Pro-substituted analogue, **23a** (Table 2). N-Methylation of D-Ala^4 in **23c** (IC_{50} = 230 nM) brought about a significant increase in potency (IC_{50} of **23d** = 42 nM), which was comparable to that of **23e** ([Ala^4]-**2**) (IC_{50} = 63 nM), while N-methylation of Ala^4 in **23e** caused a significant decrease in potency (IC_{50} of **23f** = 490 nM). NMR and simulated annealing molecular dynamics (SA-MD) analysis showed that the backbone structure of **23d** is very similar to that of **23e**, but different from that of **23c**, especially in the direction of the D-Tyr-L/D-Arg amide bond (Figure 3A).[46] N-Methylation of D-Ala^4 in **23c** might cause an inversion of the D-Tyr^3-D-Ala^4 amide bond (180° rotation of φ and ψ torsion angles) to reduce the 1,3-pseudo-allylic strain between the side chain of D-Tyr^3 and the *N*-methyl group, resulting in a conformation that is similar to that of **23e**.

Ala-substitution for Arg^4 in **2** (**23e**) did not bring about a severe decrease in potency (IC_{50} = 63 nM),

Table 2. Inhibitory Activity of Cyclic Pentapeptides with Substitution for Arg[4] in Compound **2** against SDF-1 Binding to CXCR4

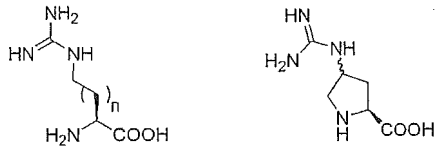

n = 1 γ-*N*-amidino-Dab (g-Dab) n = 3 ε-*N*-amidino-Lys (g-Lys)

trans/*cis*-4-guanidino-Pro

compd	sequence[a]	IC_{50} ± SD (μM)
23a	*cyclo*(-Nal-Gly-D-Tyr-D-Pro-Arg-)	1.6 ± 0.1
23b	*cyclo*(-Nal-Gly-D-Tyr-Pro-Arg-)	0.42 ± 0.29
23c	*cyclo*(-Nal-Gly-D-Tyr-D-Ala-Arg-)	0.23 ± 0.0064
23d	*cyclo*(-Nal-Gly-D-Tyr-D-MeAla-Arg-)	0.042 ± 0.0088
23e	*cyclo*(-Nal-Gly-D-Tyr-Ala-Arg-)	0.063 ± 0.013
23f	*cyclo*(-Nal-Gly-D-Tyr-MeAla-Arg-)	0.49 ± 0.090
23g	*cyclo*(-Nal-Gly-D-Tyr-Dab-Arg-)	0.016 ± 0.010
23h	*cyclo*(-Nal-Gly-D-Tyr-Orn-Arg-)	0.019 ± 0.011
23i	*cyclo*(-Nal-Gly-D-Tyr-Lys-Arg-)	0.097 ± 0.0035
23j	*cyclo*(-Nal-Gly-D-Tyr-g-Dab-Arg-)	0.024 ± 0.0040
23k	*cyclo*(-Nal-Gly-D-Tyr-g-Lys-Arg-)	0.033 ± 0.0001
23l	*cyclo*(-Nal-Gly-D-Tyr-Asn-Arg-)	0.27
23m	*cyclo*(-Nal-Gly-D-Tyr-Gln-Arg-)	0.17
23n	*cyclo*(-Nal-Gly-D-Tyr-Glu-Arg-)	0.61
23o	*cyclo*(-Nal-Gly-D-Tyr-*trans*-4-guanidino-Pro-Arg-)	0.010 ± 0.0015
23p	*cyclo*(-Nal-Gly-D-Tyr-*cis*-4-guanidino-Pro-Arg-)	0.0099 ± 0.0043

[a] MeAla = N^{α}-Me-Ala.

whereas Ala-substitution for Nal[1], D-Tyr[3], and Arg[5] completely deminished activity of the parent compound (IC_{50} > 1 μM, data not shown). These results suggest that the side chain of Arg[4] in **2** has relatively little effect on the expression of activity, and that the spatial disposition of the δ-guanidino group of Arg[4] might not be optimized. Thus, several analogues, in which Arg[4] was replaced by Arg/Lys mimetics with various lengths of alkyl chains, were synthesized. Dab/L-ornithine (Orn)-substituted analogues, **23g** and **23h**, showed higher activity (IC_{50} = 16 and 19 nM, respectively) than the Ala-substituted analogue, **23e**, whereas a Lys-substituted analogue, **23i**, was slightly weaker (IC_{50} = 97 nM) than **23e** (Table 2). γ-*N*-Amidino-Dab (g-Dab)/ε-*N*-amidino-Lys (g-Lys)-substituted analogues, **23j** and **23k**, also showed higher activity (IC_{50} = 24 and 33 nM, respectively) than **23e**. However, these analogues were weaker than compound **2**, suggesting that Arg is the most suitable at position 4 among the Arg/Lys mimetics used in this study. Asn/Gln/Glu-substituted analogues, **23l**–**n**, showed a remarkable decrease in activity (IC_{50} = 270, 170, and 610 nM, respectively). This proved that a basic functional group, such as an amino or guanidino group, is necessary for strong activity in the side chain of the amino acid at position 4, and that a hydrophilic (not basic) or acidic group is not preferable to a methyl group of Ala.

Conformationally constrained Arg mimetics, *trans*-4-guanidino-Pro and *cis*-4-guanidino-Pro (Table 2), were synthesized with the idea of fixing the backbone and side chain of Arg, according to the reported procedure.[44] These Arg mimetics were incorporated in compound **2** to determine the spatial disposition of guanidino group and increase in potency. **23o** ([*trans*-4-guanidino-Pro[4]]-**2**, *trans*-4-guanidino-Pro-substitution for Arg[4]) and **23p** ([*cis*-4-guanidino-Pro[4]]-**2**, *cis*-4-guanidino-Pro-substitution for Arg[4]) showed high CXCR4-antagonistic activities (IC_{50} = 10 and 9.9 nM, respectively) that were twice as strong as that of **23j** ([g-Dab[4]]-**2**, g-Dab-substitution for Arg[4]), having the same length of the linear-type side chain of the amino acid at position 4 (IC_{50} = 24 nM), while **23b** ([Pro[4]]-**2**, Pro-substitution for Arg[4]) did not show high activity (IC_{50} = 420 nM). In consideration of the fact that the introduction of a pyrrolidinyl ring caused a significant reduction of potency (**23a** and **23b**), it is thought that fixing the side chain effectively increased potency. From these results, we have learned that the constrained guanido group might efficiently interact with CXCR4. In addition, NMR and SA-MD analysis of **23o** and **23p** showed similar dispositions of guanidino groups of *trans*/*cis*-4-guanidino-Pro residues in space (Figure 3B),[46] which might be the reason for essentially no difference in potency between **23o** and **23p**.

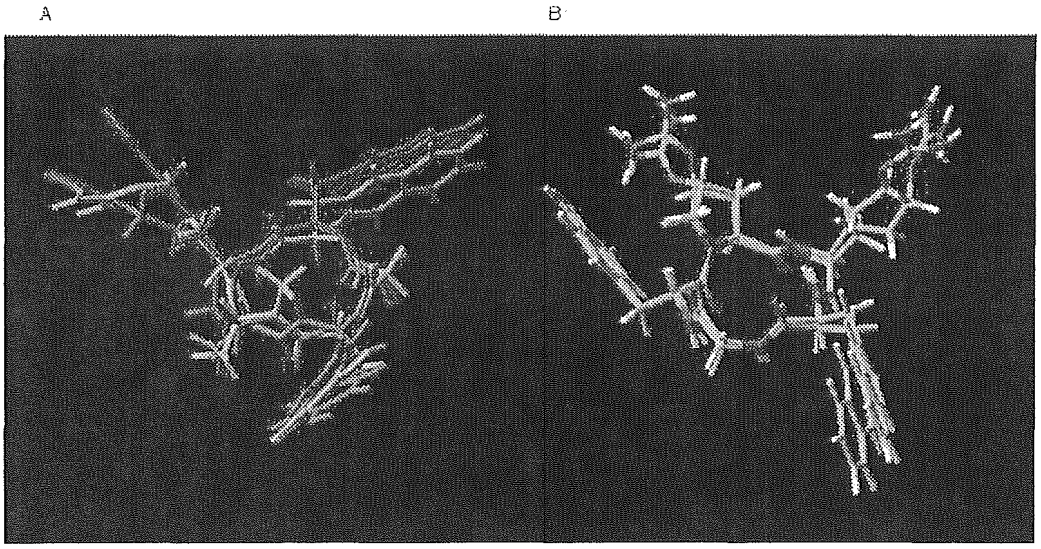

Figure 3. Superimpositions of low-energy structures of **23c** (red), **23d** (green), and **23e** (blue) (A), and **23o** and **23p** (B).

Conclusion

The fine-tuning of the ring structure of compound **2** led to findings of CXCR4 antagonists involving scaffold structures that are different from cyclic pentapeptide structures: A cyclic tetrapeptide including a γ-amino acid and pseudopeptides cyclized by disulfide and olefin bridges, having a smaller number of peptide bonds compared to compound **2**, might be useful lead compounds. Furthermore, we have learned from L/D-N^{α}-Me-Ala- and L/D-Pro-substitutions for Arg^4 that the direction of the carbonyl group in the D-Tyr^3-L/D-Ala^4 amide bonds causes a remarkable effect on CXCR4-antagonistic activity. It is also clear from this study that a basic functional group, such as amino or guanidino group, in the amino acid side-chain at position 4 is indispensable for strong activity. In addition, analogues of compound **2**, where a conformationally constrained Arg mimetic, trans- or *cis*-4-guanidino-Pro, was incorporated at position 4, showed high CXCR4-antagonistic activity, indicating that spatial constraint of a guanido group is important for an efficient interaction with CXCR4. These results for modifications of compound **2** provide useful insights for the future design of new low molecular weight CXCR4 antagonists, considering in connection with other CXCR4 antagonists.[47-53]

Experimental Section

General. ^{1}H NMR spectra were recorded using a JEOL EX-270, a JEOL AL-400, or a JNM-ECA600 spectrometer at 270, 400, or 600 MHz ^{1}H frequency, respectively, in $CDCl_3$ or DMSO-d_6. Chemical shifts are reported in parts per million downfield from internal tetramethylsilane. Nominal (LRMS) and exact mass (HRMS) spectra were recorded on a JEOL JMS-01SG-2 or JMS-HX/HX 110A mass spectrometer. Ionspray (IS)-mass spectrum was obtained with a Sciex API*III*E triple quadrupole mass spectrometer (Toronto, Canada). Optical rotations were measured in $CHCl_3$ or H_2O with a JASCO DIP-360 digital polarimeter (Tokyo, Japan) or a Horiba high-sensitive polarimeter SEPA-200 (Kyoto, Japan). For flash column chromatography, silica gel 60 H (silica gel for thin-layer chromatography, Merck) and Wakogel C-200 (silica gel for column chromatography, Wako Pure Chemical Industries, Ltd., Osaka, Japan) were employed. HPLC solvents were H_2O and CH_3CN, both containing 0.1% (v/v) TFA. For analytical HPLC, a Cosmosil 5C18-AR column (4.6 × 250 mm, Nacalai Tesque Inc., Kyoto, Japan) was eluted with a linear gradient of CH_3CN at a flow rate of 1 mL/min on a Waters model 600 (Nihon Millipore, Ltd., Tokyo, Japan). Preparative HPLC was performed on a Waters Delta Prep 4000 equipped with a Cosmosil 5C18-AR column (20 × 250 mm, Nacalai Tesque Inc.) using an isocratic mode of CH_3CN at a flow rate of 15 mL/min.

[1-(*N*,*N*-Methoxy-methyl-carbamoyl)-2(*S*)-(2-naphthyl)-ethyl]-carbamic Acid *tert*-Butyl Ester (Boc-Nal-NMe (OMe)) (4). To a stirred solution of L-3-(2-naphthyl)alanine (10.0 g, 46.4 mmol) in THF−H_2O (1:1 (v/v), 200 mL) were added triethylamine (12.5 mL, 92.9 mmol) and Boc_2O (9.63 g, 44.1 mmol) at room temperature, and the mixture was stirred at this temperature overnight. The reaction mixture was concentrated under reduced pressure. The residue was extracted with EtOAc, and the extract was washed successively with saturated aqueous citric acid, aq. 5% citric acid (× 3), H_2O (× 5), and brine and dried over $MgSO_4$. Concentration under reduced pressure gave the crude product as a white powder, which was used directly in the following step without purification. To a solution of the crude product in DMF (150 mL) were added *N*,*O*-dimethylhydroxylamine hydrochloride (10.3 g, 106 mmol), triethylamine (14.3 mL, 106 mmol), HOBt (8.11 g, 52.9 mmol), and DCC (11.8 g, 53.0 mmol) at 0 °C, and the mixture was stirred at room temperature overnight. The reaction mixture was filtered, and the filtrate was concentrated under reduced pressure. The residue was extracted with EtOAc, and the extract was washed successively with saturated aqueous citric acid, brine, saturated aqueous $NaHCO_3$, and brine and dried over $MgSO_4$. Concentration under reduced pressure followed by flash chromatography over silica gel with EtOAc−*n*-hexane (2:3) and subsequent recrystalization with Et_2O−*n*-hexane gave 12.8 g (35.7 mmol, 77% yield from L-3-(2-naphthyl)alanine) of **4** as colorless crystals. mp: 110−111 °C; $[\alpha]^{35}_D$ +29.41 (*c* 0.714, $CHCl_3$); ^{1}H NMR (400 MHz, $CDCl_3$) δ 7.73-7.82 (m, 3H), 7.62, (s, 1H), 7.39−7.48 (m, 2H), 7.31 (dd, *J* = 8.6, 1.5 Hz, 1H), 5.17−5.24 (br d, 1H), 5.06 (br, 1H), 3.66 (s, 3H), 3.01−3.25 (m, 4H), 1.36 (s, 9H); Anal. Calcd for $C_{20}H_{26}N_2O_5$: C, 67.02; H, 7.31; N, 7.82. Found: C, 66.78; H, 7.47; N, 7.68.

(2*E*,4*S*)-*N*-Boc-4-amino-5-(2-naphthyl)-2-pentenoic Acid *tert*-Butyl Ester (5). To a stirred solution of **4** (7.00 g, 19.5 mmol) in CH_2Cl_2 (50 mL) was added dropwise a solution of DIBAL-H in toluene (1.0 M, 38.6 mL, 38.6 mmol) at −78 °C under argon, and the mixture was stirred at −78 °C for 2 h. The reaction was quenched with saturated aqueous citric acid (50 mL) at −78 °C, and the organic solvents were concentrated under reduced pressure. The residue was extracted with EtOAc, and the extract was washed successively with brine, aq. 50% $NaHCO_3$, and brine and dried over $MgSO_4$. Concentration under reduced pressure gave the crude aldehyde as a white solid, which was used directly in the following step without purification. To a stirred suspension of LiCl (1.65 g, 39.0 mmol) in CH_3CN (30 mL) were added $(EtO)_2P(O)CH_2CO_2$-Bu^t (6.31 mL, 39.0 mmol) and DIPEA (6.79 mL, 39.0 mmol) at 0 °C under argon, and the mixture was stirred at 0 °C for 1 h. The above aldehyde in CH_3CN (30 mL) was added to the mixture at 0 °C, and the mixture was allowed to warm to room temperature and stirred overnight. The reaction mixture was concentrated under reduced pressure. The residue was extracted with EtOAc, and the extract was washed successively with saturated aqueous citric acid, brine, saturated aqueous $NaHCO_3$, and brine and dried over $MgSO_4$. Concentration under reduced pressure followed by flash chromatography over silica gel with EtOAc−*n*-hexane (1:4) and subsequent recrystalization with Et_2O−*n*-hexane gave 6.05 g (15.2 mmol, 78% from **4**) of **5** as colorless crystals. mp: 135−137 °C; $[\alpha]^{35}_D$ −12.84 (*c* 0.467, $CHCl_3$); ^{1}H NMR (400 MHz, $CDCl_3$) δ 7.72−7.87 (m 3H), 7.62 (s, 1H), 7.39−7.51 (m, 2H), 7.31 (dd, *J* = 8.6, 1.7 Hz, 1H), 6.85 (dd, *J* = 15.6, 5.1 Hz, 1H), 5.81 (dd, *J* = 15.6, 1.5 Hz, 1H), 4.69 (br, 1H), 4.57 (br, 1H), 2.94−3.12 (m, 2H), 1.46 (s, 9H), 1.36 (s, 9H); Anal. Calcd for $C_{24}H_{31}NO_4$: C, 72.58; H, 7.86; N, 3.52. Found: C, 72.44; H, 7.86; N, 3.22.

(2*E*,4*S*)-*N*-Fmoc-4-amino-5-(2-naphthyl)-2-pentenoic Acid (6). **5** (1.00 g, 2.51 mmol) was treated with aq. 95% TFA (20 mL) at room temperature for 2.5 h. TFA was removed under reduced pressure, and the residue was dissolved in DMF−H_2O−CH_3CN (9:1:15 (v/v), 24 mL). To the stirred solution were added DIPEA (876 μL, 5.03 mmol) and Fmoc-OSu (891 mg, 2.64 mmol) at 0 °C, and the reaction mixture was stirred at room temperature for 6 h. The mixture was concentrated under reduced pressure and acidified with aq. 1 M HCl. The mixture was extracted with EtOAc, and the extract was washed successively with aq. 0.1 M HCl (× 3) and brine and dried over $MgSO_4$. After removal of the solvent under reduced pressure, the resulting crude product was purified by flash chromatography on silica gel with $CHCl_3$−MeOH (20:1) and subsequent recrystalization with ($CHCl_3$−*n*-hexane−MeOH) to give 345.1 mg (0.753 mmol, 30% yield from **5**) of **6** as colorless crystals. mp: 189−190 °C; $[\alpha]^{34}_D$ −15.33 (*c* 0.326, $CHCl_3$); ^{1}H NMR (400 MHz, DMSO-d_6) δ 12.3 (br, 1H), 7.67−7.95 (m, 7H), 7.51−7.62 (m, 2H) 7.40−7.51 (m, 3H), 7.30−7.41 (m, 2H) 7.08−7.30 (m, 2H), 6.86 (dd, *J* = 15.6, 5.4 Hz, 1H), 5.81 (d, *J* = 15.6 Hz,1H), 4.43−4.61 (m, 1H), 4.04−4.26 (m, 3H), 3.00−3.14 (m, 1H), 2.83−3.00 (m, 1H); LRMS (FAB), *m*/*z* 464 (MH^+, base peak), 307, 179, 165, 154, 136, 141, 136, 121, 107, 91, 89, 77; HRMS (FAB), *m*/*z* calcd for $C_{30}H_{26}NO_4$ (MH^+): 464.1862, found: 464.1853.

***N*-Boc-4(*R*)-amino-5-(2-naphthyl)-pentanoic Acid *tert*-Butyl Ester (7).** To the solution of **5** (2.50 g, 6.29 mmol) in

EtOAc (100 mL) was added 10% Pd/C (200 mg). The reaction vessel was charged with atmosphere of H_2 (balloon), and the mixture was stirred at room temperature for 8 h. Completion of the reaction was monitored by RP-HPLC. The reaction mixture was filtered through a pad of Celite, rinsing with EtOAc, and the filtrate was concentrated under reduced pressure. The resulting crude product was purified by flash chromatography on silica gel with EtOAc–*n*-hexane (1:5) and subsequent recrystalization with Et_2O–*n*-hexane to give 1.87 g (4.65 mmol, 74%) of **7** as colorless crystals. mp: 90–91 °C; $[\alpha]^{35}_D$ −20.83 (c 0.432, $CHCl_3$); ^1H NMR (400 MHz, $CDCl_3$) δ 7.71–7.86 (m, 3H), 7.62 (s, 1H), 7.38–7.52 (m, 2H), 7.34 (d, J = 8.1 Hz, 2H), 4.42–4.58 (br d, 1H), 2.94–3.09 (m, 1H), 2.79–2.94 (m, 1H), 2.28 (t, 2H), 1.56–1.92 (m, 2H), 1.41 (s, 9H), 1.39 (s, 9H); Anal. Calcd for $C_{24}H_{33}NO_4$: C, 72.15; H, 8.33; N, 3.51. Found: C, 71.92; H, 8.49; N, 3.21.

***N*-Fmoc-4(*R*)-amino-5-(2-naphthyl)-pentanoic Acid (8).** **7** (1.00 g, 2.50 mmol) was treated with aq. 95% TFA (20 mL) at room temperature for 2.5 h. TFA was removed under reduced pressure, and the residue was dissolved in DMF–H_2O–THF (9:1:10 (v/v), 20 mL). To the stirred solution were added DIPEA (1.03 mL, 5.89 mmol) and Fmoc-OSu (1.29 g, 3.83 mmol) at 0 °C, and the reaction mixture was stirred at room temperature overnight. The mixture was concentrated under reduced pressure and acidified with aq. 1 M HCl. The mixture was extracted with EtOAc, and the extract was washed successively with aq. 0.1 M HCl (× 3) and brine and dried over $MgSO_4$. After removal of the solvent under reduced pressure, the resulting crude product was purified by flash chromatography on silica gel with $CHCl_3$–MeOH (20:1) and subsequent recrystalization with ($CHCl_3$–*n*-hexane) to give 747.6 mg (1.60 mmol, 64% yield from **7**) of **8** as colorless crystals. mp: 167–169 °C; $[\alpha]^{34}_D$ −7.31 (c 0.410, $CHCl_3$); ^1H NMR (400 MHz, DMSO-d_6) δ 7.73–7.92 (m 5H), 7.67 (s, 1H), 7.56–7.62 (m, 2H) 7.41–7.48 (m, 2H), 7.33–7.41 (m, 3H), 7.18–7.33 (m, 3H), 4.06–4.24 (m, 3H), 3.76 (br, 1H), 2.85 (d, J = 6.6 Hz, 2H), 2.14–2.32 (m, 2H), 1.68–1.82 (m, 1H), 1.54–1.68 (m, 1H); LRMS (FAB), *m/z* 466 (MH^+, base peak), 179, 154, 136, 141, 136; HRMS (FAB), *m/z* calcd for $C_{30}H_{23}NO_4$ (MH^+): 466.2018, found: 464.2024.

Representative Procedure for the Synthesis of γ-Amino Acid-Containing Cyclic Tetrapeptides (11a). Cl-Trt-(2-Cl) resin (1.25 mmol/g, 400 mg, 0.5 mmol) was treated with Fmoc-γ-Nal-OH (256 mg, 0.55 mmol) and DIPEA (383 μL, 2.2 mmol) in CH_2Cl_2 (4 mL) at room temperature for 2 h to yield Fmoc-γ-Nal-Trt(2-Cl) resin (0.79 mmol/g, 97%). Protected peptide **11a** resin was manually constructed by Fmoc-based solid-phase peptide synthesis on Fmoc-γ-Nal-Trt(2-Cl) resin (0.79 mmol/g, 127 mg, 0.1 mmol). But for Tyr and Pbf for Arg were employed for side-chain protection. The protected peptide **11a** resin was treated with 1,1,1,3,3,3-hexafluoro-2-propanol (HFIP)–DCM (1:4 (v/v), 7 mL) at room temperature for 2 h. After filtration, the filtrate was concentrated under reduced pressure to give the crude protected linear peptide. To a stirred mixture of the protected peptide and *N*-methylmorphorine (54.9 μL, 0.5 mmol) in DMF (25 mL) was added diphenylphosphoryl azide (DPPA) (53.2 μL, 0.247 mmol) at −40 °C. The reaction mixture was stirred for 24 h with warming up to room temperature and concentrated under reduced pressure. The residue was subjected to solid-phase extraction over basic alumina in $CHCl_3$–MeOH (9:1) to remove inorganic salts derived from DPPA. The resulting cyclic protected peptide was treated with aq. 95% TFA (10 mL) at room temperature for 2 h. Concentration under reduced pressure and purification by HPLC gave the cyclic pseudopeptide **11a** (42.9 mg, 61% yield from Fmoc-γ-Nal-Trt(2-Cl) resin) as a freeze-dried powder.

Fmoc-tyramine-Wang PEG Resin. To a mixture of Wang PEG resin (0.33 mmol/g, 1.82 g, 0.600 mmol), Fmoc-tyramine (647 mg, 1.80 mmol), Ph_3P (472 mg, 1.80 mmol), and *N*-methylmorphorine (66.0 μL, 0.600 mmol) in CH_2Cl_2–THF (3:1 (v/v), 16 mL) was added diisopropyl azodicarboxylate (DIAD) (40% solution in toluene, 886 μL, 1.80 mmol) at 0 °C. The reaction mixture was stirred at room temperature for 2 d. The obtained resin was washed with THF (20 mL × 3), DMF (20 mL × 3), MeOH (20 mL × 3), $CHCl_3$ (20 mL × 3) and Et_2O (20 mL × 3) and dried in vacuo. The loading rate of the resin was estimated by Fmoc-quantification (0.126 mmol/g (41%)).

Representative Procedure for the Synthesis of Disulfide-Bridged Cyclic Peptides (16e). Protected peptide resin was manually constructed by Fmoc-based solid-phase peptide synthesis on Fmoc-tyramine-Wang PEG resin (0.126 mmol/g, 397 mg, 0.05 mmol). Fmoc-β-Ala-OH was condensed to the N-terminal amino group of H-Cys-Arg(Pbf)-Nal-D-Cys-tyramine-Wang PEG resin, and Fmoc group was deprotected by treatment with 20% piperidine in DMF (20 min). To a mixture of the resin and DIPEA (52,5 μL, 0.300 mmol) in DMF (5 mL) was added 1*H*-pyrazole-1-carboxamidine hydrohloride (22.0 mg, 0.150 mmol) at room temperature. The reaction mixture was stirred at room temperature for 12 h. This N-guanylation procedure was repeated once again. The protected resin was treated with EDT/H_2O/TFA (2.5:2.5:95 (v/v), 6 mL) at 0 °C for 2 h. The reaction mixture was filtered, and the filtrate was concentrated by bubbling with N_2 gas. Cooled Et_2O was added to the residue, and the resulting precipitate was separated by centrifugation. The precipitate was washed with Et_2O three times. The crude peptide was dissolved in H_2O, and pH of this solution was adjusted to approximately 8 with aq. 0.28% NH_3. Air oxidation for 1 d and purification by HPLC gave the cyclic pseudopeptide **16e** (6.5 mg, 16% yield from Fmoc-tyramine-Wang PEG resin) as a freeze-dried powder.

Synthesis of 15q. Protected peptide resin was manually constructed by Fmoc-based solid-phase peptide synthesis on Fmoc-HN-Rink amide resin (0.36 mmol/g, 139 mg, 0.05 mmol). To a suspension of H-Cys-Arg(Pbf)-Nal-D-Cys-HN-Rink amide resinin DCM were added *N*-Fmoc-3-aminopropanal (44.0 mg, 0.15 mmol) and $NaBH(OAc)_3$ (53.0 mg, 0.25 mmol) at room temperature. The mixture was stirred at room-temperature overnight. Deprotection of the Fmoc group, N-guanylation, deprotection/cleavage from the resin, air oxidation, and HPLC purification were performed by use of a procedure identical with that described for the synthesis of **16e** to yield the cyclic pseudopeptide **15q** (3.0 mg, 9% yield from Fmoc-HN-Rink amide resin) as a freeze-dried powder.

Representative Procedure for the Synthesis of Olefin-Bridged Cyclic Peptides (20a). Protected peptide resin was manually constructed by Fmoc-based solid-phase peptide synthesis on Fmoc-HN-Rink amide resin (0.29 mmol/g, 172 mg, 0.05 mmol). Fmoc-β-Ala-OH was condensed to the N-terminal amino group of H-L-2-allylGly-Arg(Pbf)-Nal-D-2-allylGly-HN-Rink amide resin. To a suspension of the protected resin in dry DCM (5 mL) was added Grubbs catalyst second generation (4.20 mg, 5.00 μmol) at room temperature under argon. The reaction mixture was refluxed for 9 h. After removal of the organic solvent, this reaction was repeated once again for 12 h in the presence of the catalyst (21 mg, 0.025 mmol) in dry DCM (5 mL). The obtained resin was treated with 20% piperidine in DMF (20 min). To a mixture of the resin and DIPEA (52.5 μL, 0.300 mmol) in DMF was added 1*H*-pyrazole-1-carboxamidine hydrohloride (22.0 mg, 0.15 mmol) at room tempereture. The reaction mixture was stirred at room temperature for 12 h. This N-guanylation procedure was repeated once again. The protected resin was treated with thioanisole (940 μL), TFA (7.2 mL), and TMSBr (1.32 mL) at 0 °C for 2 h. The reaction mixture was filtered, and the filtrate was concentrated by bubbling with N_2 gas. Cooled Et_2O was added to the residue, and the resulting precipitate was separated by centrifugation. The precipitate was washed with Et_2O. The crude peptide was purified by HPLC to give the cyclic pseudopeptide **20a** (3.3 mg, 10% yield from Fmoc-HN-Rink amide resin) as a freeze-dried powder.

Representative Procedure for the Synthesis of Cyclic Pentapeptides (*cyclo*(-D-Tyr-Pro-Arg-Nal-Gly-) (23b)). Protected peptide resin was manually constructed by Fmoc-based solid-phase peptide synthesis on Fmoc-Gly-Trt(2-Cl) resin (0.741 mmol/g, 101 mg, 0.075 mmol). But for Tyr and Pbf for Arg were employed for side-chain protection. Cleavage from the resin, cyclization, deprotection, and HPLC purification were performed by use of a procedure identical with that

described for the synthesis of **11a** to yield the cyclic peptide **23b** (25.2 mg, 50% yield from Fmoc-Gly-Trt(2-Cl) resin) as a freeze-dried powder.

Representative Procedure for the Synthesis of *N*-Methylated Cyclic Pentapeptides (*cyclo*(-D-Tyr-D-MeAla-Arg-Nal-Gly-) (23d)). According to a procedure identical with that described for the preparation of **23b**, **23d** was synthesized except for N-methylation of the D-Ala residue. N-Methylation was performed by the Fukuyama–Mitsunobu reaction:[28] To a mixture of H-D-Ala-Arg(Pbf)-Nal-Gly-Trt(2-Cl) resin (0.075 mmol) and *o*-nitrobenzenesulfonyl chloride (49.9 mg, 0.225 mmol) in CH_2Cl_2 (5 mL) was added 2,4,6-collidine (49.6 μL, 0.375 mmol) at room temperature. The reaction mixture was stirred at room temperature for 2 h, and the resin was washed successively with CH_2Cl_2 (10 mL × 3) and DMF (10 mL × 3). To a mixture of the resin, Ph_3P (98.4 mg, 0.375 mmol), and MeOH (15.2 μL, 0.375 mmol) in dry THF (5 mL) was added diethyl azodicarboxylate (DEAD) (40% solution in toluene, 170 μL, 0.375 mmol) at 0 °C. The reaction mixture was stirred at room temperature for 2 h. The resin was washed successively with THF (10 mL × 3) and DMF (10 mL × 3). To a mixture of the resin and DBU (56.1 μL, 0.375 mmol) in DMF (5 mL) was added 2-mercaptoethanol (51.4 μL, 0.750 mmol) at room temperature, and the reaction mixture was stirred at room temperature for 2 h. Subsequent condensation of the next residue (D-Tyr) to the secondary amino group on the resin was performed by treatment with Fmoc-D-Tyr(Bu^t)-OH (5 equiv), HATU (4.9 equiv), HOAt (5 equiv), and DIPEA (10 equiv) in DMF (5 mL) for 1 h (× 2). **23d** (freeze-dried powder): 3.0 mg, 6.0% yield from Fmoc-Gly-Trt(2-Cl) resin.

(2*S*,4*S*)-*N*$^\alpha$-Cbz-4-*N*-Boc-aminoproline Benzyl Ester. (2*S*,4*S*)-*N*$^\alpha$-Cbz-4-aminoproline benzyl ester (1.44 g, 3.93 mmol), which was prepared from (2*S*,4*S*)-*N*$^\alpha$-Cbz-4-azidoproline benzyl ester according to Tamaki's procedure,[35] was dissolved in THF (20 mL), and Boc_2O (1.38 g, 6.31 mmol) and triethylamine (1.10 mL, 7.89 mmol) were added to the solution at 0 °C. The reaction mixture was stirred at room temperature for 7.5 h. The mixture was concentrated under reduced pressure, and the residue was extracted with Et_2O. The extract was washed successively with saturated aqueous citric acid (× 2), H_2O (× 2), and brine and dried over $MgSO_4$. After removal of the solvent under reduced pressure, the resulting crude product was purified by flash chromatography on silica gel with EtOAc–*n*-hexane (1:4) to give 1.70 g (3.77 mmol, 96% yield) of the title compound as a colorless oil. $[\alpha]^{29}_D$ −39.47 (*c* 0.304, $CHCl_3$); ^{1}H NMR (400 MHz, $CDCl_3$) δ 7.18–7.45 (m, 10H), 4.95–5.40 (m, 5H), 4.28–4.50 (m, 2H), 3.68–3.82 (m, 1H), 3.44–3.60 (m, 1H), 2.39–2.57 (m, 1H), 1.89–2.05 (m, 1H), 1.45 (s, 9H); LRMS (FAB), *m/z* 477 (MNa^+, base peak), 455 (MH^+), 445, 399, 355, 91; HRMS (FAB), *m/z* calcd for $C_{25}H_{31}N_2O_6$ (MH^+): 455.2182, found: 455.2186.

(2*S*,4*S*)-*N*$^\alpha$-Fmoc-4-*N*-Boc-aminoproline. (2*S*,4*S*)-*N*$^\alpha$-Cbz-4-*N*-Boc-aminoproline benzyl ester (1.70 g, 3.77 mmol) was dissolved in EtOH (80 mL), and 5% Pd/C (170 mg) was added to the solution. The reaction vessel was charged with atmosphere of H_2 (balloon), and the mixture was stirred at room temperature for 12 h. After removal of Pd/C by filtration, the filtrate was concentrated under reduced pressure to give the crude product as a colorless oil, which was used directly in the following step without purification. To the crude product in H_2O–THF (4:3 (v/v), 70 mL) were added triethylamine (1.41 mL, 7.55 mmol) and Fmoc-OSu (2.54 g, 7.55 mmol) in CH_3CN (10 mL) at 0 °C, and the reaction mixture was stirred at room temperature for 2 h. The mixture was acidified with saturated aqueous citric acid and concentrated under reduced pressure. The residue was extracted with EtOAc, and the extract was washed successively with saturated aqueous citric acid, H_2O (× 3), and brine and dried over $MgSO_4$. After removal of the solvent under reduced pressure, the resulting crude product was purified by flash chromatography on silica gel with $CHCl_3$–MeOH (20:1) to give 1.18 g (2.60 mmol, 69% yield) of the title compound as colorless crystals. mp: 87–89 °C; $[\alpha]^{24}_D$ −33.81 (*c* 0.621, $CHCl_3$); ^{1}H NMR (400 MHz, DMSO-d_6) δ 8.30 (s, 1H), 7.82–7.97 (m, 2H), 7.57–7.75 (m, 2H), 7.25–7.49 (m, 4H), 3.93–4.36 (m, 5H), 3.60–3.75 (m, 1H), 3.05–3.21 (m, 1H), 2.32–2.58 (m, 1H), 1.67–1.90 (m, 1H), 1.44 (s, 9H); LRMS (FAB), *m/z* 451 [(M − H)$^-$], 229, 155, 153, 152 (base peak); HRMS (FAB), *m/z* calcd for $C_{25}H_{27}N_2O_6$ [(M − H)$^-$]: 451.1868, found: 451.1883.

(2*S*,4*R*)-*N*$^\alpha$-Cbz-4-*N*-Boc-aminoproline Benzyl Ester. By use of a procedure identical with that described for the preparation of (2*S*,4*S*)-*N*$^\alpha$-Cbz-4-*N*-Boc-aminoproline benzyl ester, (2*S*,4*R*)-*N*$^\alpha$-Cbz-4-aminoproline benzyl ester (5.56 g, 15.7 mmol) was converted into 6.24 g (13.8 mmol, 88% yield) of the title compound as colorless crystals. mp: 97–99 °C; $[\alpha]^{25}_D$ −47.61 (*c*, 0.714, $CHCl_3$); ^{1}H NMR (400 MHz, $CDCl_3$) δ 7.15–7.43 (m, 10H), 4.93–5.27 (m, 4H), 4.56–4.70 (br, 1H), 4.37–4.54 (m, 1H), 4.21–4.35 (br, 1H), 3.78–3.89 (m, 1H), 3.30–3.50 (m, 1H), 2.12–2.34 (m, 2H), 1.45 (s, 9H); LRMS (FAB), *m/z* 477 (MNa^+, base peak), 455 (MH^+), 445, 399, 355, 263, 91; HRMS (FAB), *m/z* calcd for $C_{25}H_{31}N_2O_6$ (MH^+): 455.2182, found: 455.2176.

(2*S*,4*R*)-*N*$^\alpha$-Fmoc-4-*N*-Boc-aminoproline. By use of a procedure identical with that described for the preparation of (2*S*,4*S*)-*N*$^\alpha$-Fmoc-4-*N*-Boc-aminoproline, (2*S*,4*R*)-*N*$^\alpha$-Cbz-4-*N*-Boc-aminoproline benzyl ester (2.75 g, 6.10 mmol) was converted into 2.05 g (4.51 mmol, 74% yield) of the title compound as colorless crystals. mp: 85–87 °C; $[\alpha]^{24}_D$ −36.92 (*c* 0.325, $CHCl_3$); ^{1}H NMR (400 MHz, $CDCl_3$) δ 8.33 (s, 1H), 7.82–7.97 (m, 2H), 7.56–7.72 (m, 2H), 7.26–7.49 (m, 4H), 3.96–4.36 (m, 4H), 3.50–3.67 (m, 1H), 3.18–3.40 (m, 2H), 1.99–2.26 (m, 2H), 1.44 (s, 9H); LRMS (FAB), *m/z* 451 [(M − H)$^-$], 229, 155, 153, 151 (base peak); HRMS (FAB), *m/z* calcd for $C_{25}H_{27}N_2O_6$ [(M − H)$^-$]: 451.1868, found: 451.1887.

Representative Procedure for the Synthesis of Cyclic Pentapeptides Containing Arginine Mimetic (*cyclo*(-D-Tyr-*trans*-4-guanidino-Pro-Arg-Nal-Gly-) (23o)). According to a procedure identical with that described for the preparation of **23b**, the cyclic protected peptide was synthesized. The obtained protected peptide (0.05 mmol) was treated with aq. 95% TFA (5 mL) for 2 h at room temperature, and concentration under reduced pressure gave the crude cyclic peptide. To a mixture of the crude product and 1*H*-pyrazole-1-carboxamidine hydrochloride (22.0 mg, 0.15 mmol) in DMF (4 mL) was added DIPEA (52.3 μL, 0.300 mmol) at room temperature. The reaction mixture was stirred at room temperature for 12 h. This procedure (N-guanylation of the γ-amino group of the *trans*-4-amino-Pro residue) was repeated once again. Concentration under reduced pressure and purification by HPLC gave the cyclic peptide **23o** (5.1 mg, 14% yield from Fmoc-Gly-Trt(2-Cl) resin) as a freeze-dried powder.

[^{125}I]-SDF-1 Binding and Displacement. Stable CHO cell transfectants expressing CXCR4 variants were prepared as described previously.[54] CHO transfectants were harvested by treatment with trypsin-EDTA, allowed to recover in complete growth medium (MEM-α, 100 μg/mL penicillin, 100 μg/mL streptomycin, 0.25 μg/mL amphotericin B, 10% (v/v)) for four to 5 h and then washed in cold binding buffer (PBS containing 2 mg/mL BSA). For ligand binding, the cells were resuspended in binding buffer at 1 × 10^7 cells/mL, and 100 μL aliquots were incubated with 0.1 nM of [^{125}I]-SDF-1 (PerkinElmer Life Sciences) for 2 h on ice under constant agitation. Free and bound radioactivity were separated by centrifugation of the cells through an oil cushion and bound radioactivity was measured with a gamma-counter (Cobra, Packard, Downers Grove, IL). Inhibitory activity of test compounds was determined based on the inhibition of [^{125}I]-SDF-1-binding to CXCR4 transfectants (IC_{50}).

NMR Spectroscopy (23c–e, 23o, and 23p). The peptide sample was dissolved in DMSO-d_6 at a concentration of 5 mM. ^{1}H NMR spectra of the peptides were recorded at 300 K. The assignments of the proton resonances were achieved by use of ^{1}H–^{1}H COSY spectra. $^3J(H^N,H^\alpha)$ coupling constants were measured from one-dimensional spectra. The mixing time for the NOESY experiments was set at 400 ms. NOESY spectra were composed of 512 real points in the F2 dimension and 256 real points, which were zero-filled to 256 points in the F1 dimension, with 144 scans per t1 increment. The cross-peak

intensities were evaluated by relative build-up rates of the cross-peaks. Temperature dependence of the chemical shifts of all of the amide protons was investigated in **23c**−**e**, **23o**, and **23p**. In **23c**, the temperature coefficients for all of the NH protons were large. In **23d**, the only temperature coefficient for the NH of D-Tyr^3 was small, but NOE was not observed between the Nal^1 C$^\alpha$H and D-Tyr^3 NH. In **23e**, **23o**, and **23p**, the temperature coefficients for the NH of D-Tyr^3 and Arg^5 were small, but NOE was not observed between the Nal^1 C$^\alpha$H and D-Tyr^3 NH or between the D-Tyr^3 C$^\alpha$H and Arg^5 NH. Thus, no hydrogen bond restraints were used in the simulated annealing calculations of **23c**−**e**, **23o**, and **23p**.

Calculation of Structures. The structure calculations were performed on a Silicon Graphics Origin 2000 workstation with the NMR-refine program within the Insight II/Discover package using the consistent valence force field (CVFF).[55] Pseudoatoms were defined for the methylene protons of Nal^1, D-Tyr^3, Arg^4, and Arg^5 prochiralities of which were not identified by ^{1}H NMR data. The restraints, in which the Gly^2 α-methylene participated, were defined for the separate protons without definition of the prochiralities. The dihedral ϕ angle constraints were calculated based on the Karplus equation: $^3J(H^N,H^\alpha) = 6.7\cos^2(\theta - 60) - 1.3\cos(\theta - 60) + 1.5$.[56] Lower and upper angle errors were set to 15°. The NOESY spectrum with a mixing time of 400 ms was used for the estimation of the distance restraints between protons. The NOE intensities were classified into three categories (strong, medium, and weak) based on the number of contour lines in the cross-peaks to define the upper-limit distance restraints (2.7, 3.5, and 5.0 Å, respectively). The upper-limit restraints were increased by 1.0 Å for the involved pseudoatoms. Lower bounds between nonbonded atoms were set to their van der Waals radii (1.8 Å). These distance and dihedral angle restraints were included with force constants of 25−100 kcal/mol·Å^2 and 25−100 kcal/mol·rad^2, respectively. The 50 initial structures generated by the NMR refine program randomly were subjected to the simulated annealing calculations. The final minimization stage was achieved until the maximum derivative became less than 0.01 kcal/mol·Å^2 by the steepest descents and conjugate gradients methods.

Acknowledgment. This work was supported in part by a 21st Century COE Program "Knowledge Information Infrastructure for Genome Science", a Grant-in-Aid for Scientific Research from the Ministry of Education, Culture, Sports, Science and Technology, Japan, and the Japan Health Science Foundation. Computation time was provided by the Supercomputer Laboratory, Institute for Chemical Research, Kyoto University. S.U. is grateful for a Research Fellowship from the Japan Society for the Promotion of Science for Young Scientists.

Supporting Information Available: Characterization data of representative synthetic compounds and HPLC charts of **11a**, **11c**, **15e**, **16e**, **15q**, **16q**, **20a**, **20d**, **23d**, **23j**, **23o**, and **23p**. This material is available free of charge via the Internet at http://pubs.acs.org.

References

(1) Nagasawa, T.; Kikutani, H.; Kishimoto, T. Molecular cloning and structure of a pre-B-cell growth-stimulating factor. *Proc. Natl. Acad. Sci. U.S.A.* **1994**, *91*, 2305−2309.
(2) Bleul, C. C.; Farzan, M.; Choe, H.; Parolin, C.; Clark-Lewis, I.; Sodroski, J.; Springer, T. A. The lymphocyte chemoattractant SDF-1 is a ligand for LESTR/fusin and blocks HIV-1 entry. *Nature* **1996**, *382*, 829−833.
(3) Oberlin, E.; Amara, A.; Bachelerie, F.; Bessia, C.; Virelizier, J.-L.; Arenzana-Seisdedos, F.; Schwartz, O.; Heard, J.-M.; Clark-Lewis, I.; Legler, D. F.; Loetscher, M.; Baggiolini, M.; Moser, B. The CXC chemokine SDF-1 is the ligand for LESTR/fusin and prevents infection by T-cell-line-adapted HIV-1. *Nature* **1996**, *382*, 833−835.
(4) Tashiro, K.; Tada, H.; Heilker, R.; Shirozu, M.; Nakano, T.; Honjo, T. Signal sequence trap: a cloning strategy for secreted proteins and type I membrane proteins. *Science* **1993**, *261*, 600−603.
(5) Feng, Y.; Broder, C. C.; Kennedy, P. E.; Berger, E. A. HIV-1 entry co-factor: Functional cDNA cloning of a seven-transmembrane, G protein-coupled receptor. *Science* **1996**, *272*, 872−877.
(6) Müller, A.; Homey, B.; Soto, H.; Ge, N.; Catron, D.; Buchanan, M. E.; McClanahan, T.; Murphy, E.; Yuan, W.; Wagner, S. N.; Barrera, J. L.; Mohar, A.; Verastegui, E.; Zlotnik, A. Involvement of chemokine receptors in breast cancer metastasis. *Nature* **2001**, *410*, 50−56.
(7) Koshiba, T.; Hosotani, R.; Miyamoto, Y.; Ida, J.; Tsuji, S.; Nakamura, S.; Kawaguchi, M.; Kobayashi, H.; Doi, R.; Hori, T.; Fujii, N.; Imamura, M. Expression of stromal cell-derived factor 1 and CXCR4 ligand receptor system in pancreatic cancer: a possible role for tumor progression. *Clin. Cancer Res.* **2000**, *6*, 3530−3535.
(8) Mori, T.; Doi, R.; Koizumi, K.; Toyoda, E.; Tulachan, S. S.; Ito, D.; Kami, K.; Masui, T.; Fujimoto, K.; Tamamura, H.; Hiramatsu, K.; Fujii, N.; Imamura, M. CXCR4 antagonist inhibits stromal cell-derived factor 1-induced migration and invasion of human pancreatic cancer. *Mol. Cancer Ther.* **2004**, *3*, 29−37.
(9) Robledo, M. M.; Bartolome, R. A.; Longo, N.; Miguel Rodriguez-Frade, J.; Mellado, M.; Longo, I.; van Muijen, G. N. P.; Sanchez-Mateos, P.; Teixido, J. Expression of functional chemokine receptors CXCR3 and CXCR4 on human melanoma cells. *J. Biol. Chem.* **2001**, *276*, 45098−45105.
(10) Taichman, R. S.; Cooper, C.; Keller, E. T.; Pienta, K. J.; Taichman, N. S.; McCauley, L. K. Use of the stromal cell-derived factor-1/CXCR4 pathway in prostate cancer metastasis to bone. *Cancer Res.* **2002**, *62*, 1832−1837.
(11) Schrader, A. J.; Lechner, O.; Templin, M.; Dittmar, K. E. J.; Machtens, S.; Mengel, M.; Probst-Kepper, M.; Franzke, A.; Wollensak, T.; Gatzlaff, P.; Atzpodien, J.; Buer, J.; Lauber, J. CXCR4/CXCL12 expression and signalling in kidney cancer. *Br. J. Cancer* **2002**, *86*, 1250−1256.
(12) Geminder, H.; Sagi-Assif, O.; Goldberg, L.; Meshel, T.; Rechavi, G.; Witz, I. P.; Ben-Baruch, A. A possible role for CXCR4 and its ligand, the CXC chemokine stromal cell-derived factor-1, in the development of bone marrow metastases in neuroblastoma. *J. Immunol.* **2001**, *167*, 4747−4757.
(13) Bertolini, F.; Dell'Agnola, C.; Mancuso, P.; Rabascio, C.; Burlini, A.; Monestiroli, S.; Gobbi, A.; Pruneri, G.; Martinelli, G. CXCR4 neutralization, a novel therapeutic approach for non-Hodgkin's lymphoma. *Cancer Res.* **2002**, *62*, 3106−3112.
(14) Kijima, T.; Maulik, G.; Ma, P. C.; Tibaldi, E. V.; Turner, R. E.; Rollins, B.; Sattler, M.; Johnson, B. E.; Salgia, R. Regulation of cellular proliferation, cytoskeletal function, and signal transduction through CXCR4 and c-Kit in small cell lung cancer cells. *Cancer Res.* **2002**, *62*, 6304−6311.
(15) Scotton, C. J.; Wilson, J. L.; Milliken, D.; Stamp, G.; Balkwill, F. R. Epithelial cancer cell migration: a role for chemokine receptors? *Cancer Res.* **2001**, *61*, 4961−4965.
(16) Scotton, C. J.; Wilson, J. L.; Scott, K.; Stamp, G.; Wilbanks, G. D.; Fricker, S.; Bridger, G.; Balkwill, F. R. Multiple actions of the chemokine CXCL12 on epithelial tumor cells in human ovarian cancer. *Cancer Res.* **2002**, *62*, 5930−5938.
(17) Sanz-Rodriguez, F.; Hidalgo, A.; Teixido, J. Chemokine stromal cell-derived factor-1α modulates VLA-4 integrin-mediated multiple myeloma cell adhesion to CS-1/fibronectin and VCAM-1. *Blood* **2001**, *97*, 346−351.
(18) Tsukada, N.; Burger, J. A.; Zvaifler, N. J.; Kipps, T. J. Distinctive features of "nurselike" cells that differentiate in the context of chronic lymphocytic leukemia. *Blood* **2002**, *99*, 1030−1037.
(19) Juarez, J.; Bradstock, K. F.; Gottlieb, D. J.; Bendall, L. J. Effects of inhibitors of the chemokine receptor CXCR4 on acute lymphoblastic leukemia cells in vitro. *Leukemia* **2003**, *17*, 1294−1300.
(20) Rubin, J. B.; Kung, A. L.; Klein, R. S.; Chan, J. A.; Sun, Y.-P.; Schmidt, K.; Kieran, M. W.; Luster, A. D.; Segal, R. A. A small-molecule antagonist of CXCR4 inhibits intracranial growth of primary brain tumors. *Proc. Natl. Acad. Sci. U.S.A.* **2003**, *100*, 13513−13518.
(21) Nanki, T.; Hayashida, K.; El-Gabalawy, H. S.; Suson, S.; Shi, K.; Girschick, H. J.; Yavuz, S.; Lipsky, P. E. Stromal cell-derived factor-1-CXC chemokine receptor 4 interactions play a central role in CD4$^+$ T cell accumulation in rheumatoid arthritis synovium. *J. Immunol.* **2000**, *165*, 6590−6598.
(22) Tamamura, H.; Xu, Y.; Hattori, T.; Zhang, X.; Arakaki, R.; Kanbara, K.; Omagari, A.; Otaka, A.; Ibuka, T.; Yamamoto, N.; Nakashima, H.; Fujii, N. A low molecular weight inhibitor against the chemokine receptor CXCR4: a strong anti-HIV peptide T140. *Biochem. Biophys. Res. Commun.* **1998**, *253*, 877−882.
(23) Tamamura, H.; Hori, A.; Kanzaki, N.; Hiramatsu, K.; Mizumoto, M.; Nakashima, H.; Yamamoto, N.; Otaka, A.; Fujii, N. T140 analogs as CXCR4 antagonists identified as anti-metastatic agents in the treatment of breast cancer. *FEBS Lett.* **2003**, *550*, 79−83.

(24) Tamamura, H.; Fujisawa, M.; Hiramatsu, K.; Mizumoto, M.; Nakashima, H.; Yamamoto, N.; Otaka, A.; Fujii, N. Identification of a CXCR4 antagonist, a T140 analog, as an anti-rheumatoid arthritis agent. *FEBS Lett.* **2004**, *569*, 99−104.
(25) Tamamura, H.; Omagari, A.; Oishi, S.; Kanamoto, T.; Yamamoto, N.; Peiper, S. C.; Nakashima, H.; Otaka, A.; Fujii, N. Pharmacophore identification of a specific CXCR4 inhibitor, T140, leads to development of effective anti-HIV agents with very high selectivity indexes. *Bioorg. Med. Chem. Lett.* **2000**, *10*, 2633−2637.
(26) Fujii, N.; Oishi, S.; Hiramatsu, K.; Araki, T.; Ueda, S.; Tamamura, H.; Otaka, A.; Kusano, S.; Terakubo, S.; Nakashima, H.; Broach, J. A.; Trent, J. O.; Wang, Z.; Peiper, S. C. Molecular-size reduction of a potent CXCR4-chemokine antagonist using orthogonal combination of conformation- and sequence-based libraries. *Angew. Chem., Int. Ed.* **2003**, *42*, 3251−3253.
(27) Fukami, T.; Nagase, T.; Fujita, K.; Hayama, T.; Niiyama, K.; Mase, T.; Nakajima, S.; Fukuroda, T.; Saeki, T.; Nishikibe, M.; Ihara, M.; Yano, M.; Ishikawa, K. Structure−activity relationships of cyclic pentapeptide endothelin A receptor antagonists. *J. Med. Chem.* **1995**, *38*, 4309−4324.
(28) Haubner, R.; Gratias, R.; Diefenbach, B.; Goodman, S. L.; Jonczyk, A.; Kessler, H. Structural and functional aspects of RGD-containing cyclic pentapeptides as highly potent and selective integrin $\alpha V\beta 3$ antagonists. *J. Am. Chem. Soc.* **1996**, *118*, 7461−7472.
(29) Spatola, A. F.; Crozet, Y.; deWit, D.; Yanagisawa, M. Rediscovering an endothelin antagonist (BQ-123): A self-deconvoluting cyclic pentapeptide library. *J. Med. Chem.* **1996**, *39*, 3842−3846.
(30) Wermuth, J.; Goodman, S. L.; Jonczyk, A.; Kessler, H. Stereoisomerism and biological activity of the selective and superactive $\alpha V\beta 3$ integrin inhibitor cyclo(−RGDfV-) and its retro-inverso peptide. *J. Am. Chem. Soc.* **1997**, *119*, 1328−1335.
(31) Haubner, R.; Finsinger, D.; Kessler, H. Stereoisomeric peptide libraries and peptidomimetics for designing selective inhibitors of the $\alpha V\beta 3$ integrin for a new cancer therapy. *Angew. Chem., Int. Ed. Engl.* **1997**, *36*, 1374−1389.
(32) Porcelli, M.; Casu, M.; Lai, A.; Saba, G.; Pinori, M.; Cappelletti, S.; Mascagni, P. Cyclic pentapeptides of chiral sequence DLDDL as scaffold for antagonism of G-protein coupled receptors: Synthesis, activity and conformational analysis by NMR and molecular dynamics of ITF 1565 a substance P inhibitor. *Biopolymers* **1999**, *50*, 211−219.
(33) Oishi, S.; Kamano, T.; Niida, A.; Odagaki, Y.; Hamanaka, N.; Yamamoto, M.; Ajito, K.; Tamamura, H.; Otaka, A.; Fujii, N. Diastereoselective synthesis of new ψ[(*E*)-CH=CMe]- and ψ-[(*Z*)-CH=CMe]-type alkene dipeptide isosteres by organocopper reagents and application to conformationally restricted cyclic RGD peptidomimetics. *J. Org. Chem.* **2002**, *67*, 6162−6173.
(34) Nikiforovich, G. V.; Kover, K. E.; Zhang, W.-J.; Marshall, G. R. Cyclopentapeptides as flexible conformational templates. *J. Am. Chem. Soc.* **2000**, *122*, 3262−3273.
(35) Tamamura, H.; Hiramatsu, K.; Ueda, S.; Wang, Z.; Kusano, S.; Terakubo, S.; Trent, J. O.; Peiper, S. C.; Yamamoto, N.; Nakashima, H.; Otaka, A.; Fujii, N. Stereoselective synthesis of [L-Arg-L/D-3-(2-naphthyl)alanine]-type (*E*)-alkene dipeptide isosteres and its application to the synthesis and biological evaluation of pseudopeptide analogues of the CXCR4 antagonist FC131. *J. Med. Chem.* **2005**, *48*, 380−391.
(36) Abdel-Magid, A. F.; Maryanoff, C. A.; Carson, K. G. Reductive amination of aldehydes and ketones by using sodium triacetoxyborohydride. *Tetrahedron Lett.* **1990**, *31*, 5595−5598.
(37) Fukuyama, T.; Jow, C.-K.; Cheung, M. 2- and 4-Nitrobenzenesulfonamides: exceptionally versatile means for preparation of secondary amines and protection of amines. *Tetrahedron Lett.* **1995**, *36*, 6373−6374.
(38) Myers, A. G.; Gleason, J. L.; Yoon, T.; Kung, D. W. Highly practical methodology for the synthesis of D- and L-*R*-amino acids, N-protected *R*-amino acids, and *N*-methyl-*R*-amino acids. *J. Am. Chem. Soc.* **1997**, *119*, 656−673.
(39) Travins, J. M.; Etzkorn, F. A. Facile synthesis of D-amino acids from an L-serine-derived aziridine. *Tetrahedron Lett.* **1998**, *39*, 9389−9392.
(40) Biagini, S. C. G.; Gibson, S. E.; Keen, S. P. Cross-metathesis of unsaturated α-amino acid derivatives. *J. Chem. Soc., Perkin. Trans. 1* **1998**, 2485−2499.
(41) Oppolzer, W.; Lienard, P. Non-destructive cleavage of *N*-acylsultams under neutral conditions: preparation of enantiomerically pure, Fmoc-protected α-amino acids. *Helv. Chim. Acta* **1992**, *75*, 2572−2582.
(42) Douat, C.; Heitz, A.; Martinez, J.; Fehrentz, J.-A. Stereoselective synthesis of allyl- and homoallylglycines. *Tetrahedron Lett.* **2001**, *42*, 3319−3321.
(43) Scholl, M.; Ding, S.; Lee, C. W.; Grubbs, R. H. Synthesis and activity of a new generation of ruthenium-based olefin metathesis catalysts coordinated with 1,3-dimesityl-4,5-dihydroimidazol-2-ylidene ligands. *Org. Lett.* **1999**, *1*, 953−956.
(44) Tamaki, M.; Han, G.; Hruby, V. J. Practical and efficient synthesis of orthogonally protected constrained 4-guanidinoprolines. *J. Org. Chem.* **2001**, *66*, 1038−1042.
(45) Tamamura, H.; Sugioka, M.; Odagaki, Y.; Omagari, A.; Kan, Y.; Oishi, S.; Nakashima, H.; Yamamoto, N.; Peiper, S. C.; Hamanaka, N.; Otaka, A.; Fujii, N. Conformational study of a highly specific CXCR4 inhibitor, T140, disclosing the close proximity of its intrinsic pharmacophores associated with strong anti-HIV activity. *Bioorg. Med. Chem. Lett.* **2001**, *11*, 359−362 and 2409.
(46) Intramolecular hydrogen bonds were not observed in the calculated structures of these cyclic pentapeptides. Thus, these peptides do not seem to exist in a characteristic turn conformation such as a βII′γ turn as reported in several papers concerning normal cyclic pentapeptides, see Weisshoff, H.; Prasang, C.; Henklein, P.; Frommel, C.; Zschunke, A.; Mugge, C. Mimicry of βII′-turns of proteins in cyclic pentapeptides with one and without D-amino acids. *Eur. J. Biochem.* **1999**, *259*, 776−788.
(47) Murakami, T.; Nakajima, T.; Koyanagi, Y.; Tachibana, K.; Fujii, N.; Tamamura, H.; Yoshida, N.; Waki, M.; Matsumoto, A.; Yoshie, O.; Kishimoto, T.; Yamamoto, N.; Nagasawa, T. A small molecule CXCR4 inhibitor that blocks T cell line-tropic HIV-1 infection. *J. Exp. Med.* **1997**, *186*, 1389−1393.
(48) Schols, D.; Struyf, S.; Van Damme, J.; Este, J. A.; Henson, G.; De Clercq, E. Inhibition of T-tropic HIV strains by selective antagonization of the chemokine receptor CXCR4. *J. Exp. Med.* **1997**, *186*, 1383−1388.
(49) Donzella, G. A.; Schols, D.; Lin, S. W.; Este J. A.; Nagashima, K. A.; Maddon, P. J.; Allaway, G. P.; Sakmar, T. P.; Henson, G.; De Clercq, E.; Moore, J. P. AMD3100, a small molecule inhibitor of HIV-1 entry via the CXCR4 co-receptor. *Nat. Med.* **1998**, *4*, 72−77.
(50) Doranz, B. J.; Grovit-Ferbas, K.; Sharron, M. P.; Mao, S.-H.; Bidwell Goetz, M.; Daar, E. S.; Doms, R. W.; O'Brien, W. A. A small-molecule inhibitor directed against the chemokine receptor CXCR4 prevents its use as an HIV-1 coreceptor. *J. Exp. Med.* **1997**, *186*, 1395−1400.
(51) Howard, O. M. Z.; Oppenheim, J. J.; Hollingshead, M. G.; Covey, J. M.; Bigelow, J.; McCormack, J. J.; Buckheit, Jr., R. W.; Clanton, D. J.; Turpin, J. A.; Rice, W. G. Inhibition of in vitro and in vivo HIV replication by a distamycin analogue that interferes with chemokine receptor function: a candidate for chemotherapeutic and microbicidal application. *J. Med. Chem.* **1998**, *41*, 2184−2193.
(52) Fujii, N.; Nakashima, H.; Tamamura, H. The Therapeutic Potential of CXCR4 Antagonists in the Treatment of HIV. *Expert Opin. Investig. Drugs* **2003**, *12*, 185−195.
(53) Tamamura, H.; Fujii, N. Two Orthogonal Approaches to Overcome Multi-Drug Resistant HIV-1s: Development of Protease Inhibitors and Entry Inhibitors Based on CXCR4 Antagonists. *Curr. Drug Targets-Infect. Disord.* **2004**, *4*, 103−110.
(54) Navenot, J. M.; Wang , Z. X.; Trent, J. O.; Murray, J. L.; Hu, Q. X.; DeLeeuw, L.; Moore, P. S.; Chang, Y.; Peiper, S. C. Molecular anatomy of CCR5 engagement by physiologic and viral chemokines and HIV-1 envelope glycoproteins: Differences in primary structural requirements for RANTES, MIP-1α, and vMIP−II binding. *J. Mol. Biol.* **2001**, *313*, 1181−1193.
(55) Miyamoto, K.; Nakagawa, T.; Kuroda, Y. Solution structure of the cytoplasmic linker between domain III−S6 and domain IV−S1 (III−IV linker) of the rat brain sodium channel in SDS micelles. *Biopolymers* **2001**, *59*, 380−393.
(56) Ludvigsen, S.; Andersen, K. V.; Poulsen, F. M. Accurate measurements of coupling-constants from 2-dimensional nuclear-magnetic-resonance spectra of proteins and determination of ϕ-angles *J. Mol. Biol.* **1991**, *217*, 731−736.

JM050009H

JOURNAL OF VIROLOGY, Feb. 2005, p. 1452–1462 Vol. 79, No. 3
0022-538X/05/$08.00+0 doi:10.1128/JVI.79.3.1452–1462.2005

Vaccination of Rhesus Macaques with Recombinant *Mycobacterium bovis* Bacillus Calmette-Guérin Env V3 Elicits Neutralizing Antibody-Mediated Protection against Simian-Human Immunodeficiency Virus with a Homologous but Not a Heterologous V3 Motif

Kenji Someya,[1]* Dayaraj Cecilia,[2] Yasushi Ami,[3] Tadashi Nakasone,[1] Kazuhiro Matsuo,[1,4] Sherri Burda,[2] Hiroshi Yamamoto,[5] Naoto Yoshino,[6] Masahiko Kaizu,[1,4] Shuji Ando,[1] Kenji Okuda,[7] Susan Zolla-Pazner,[2] Shudo Yamazaki,[1] Naoki Yamamoto,[1] and Mitsuo Honda[1,4]

AIDS Research Center[1] and Division of Experimental Animal Research,[3] National Institute of Infectious Diseases, Shinjuku-ku, Tokyo, Yokohama City University, Kanazawa-ku, Yokohama,[7] Japan Science and Technology Corporation, Kawaguchi, Saitama,[4] Toyama Medical Pharmaceutical University, Toyama, Toyama,[5] and Iwate Medical University, Morioka, Iwate,[6] Japan, and New York University Medical Center, New York, New York[2]

Received 25 June 2004/Accepted 23 September 2004

Although the correlates of vaccine-induced protection against human immunodeficiency virus type 1 (HIV-1) are not fully known, it is presumed that neutralizing antibodies (NAb) play a role in controlling virus infection. In this study, we examined immune responses elicited in rhesus macaques following vaccination with recombinant *Mycobacterium bovis* bacillus Calmette-Guérin expressing an HIV-1 Env V3 antigen (rBCG Env V3). We also determined the effect of vaccination on protection against challenge with either a simian-human immunodeficiency virus (SHIV-MN) or a highly pathogenic SHIV strain (SHIV-89.6PD). Immunization with rBCG Env V3 elicited significant levels of NAb for the 24 weeks tested that were predominantly HIV-1 type specific. Sera from the immunized macaques neutralized primary HIV-1 isolates in vitro, including HIV-$1_{BZ167/X4}$, HIV-$1_{SF2/X4}$, HIV-$1_{CI2/X4}$, and, to a lesser extent, HIV-$1_{MNp/X4}$, all of which contain a V3 sequence homologous to that of rBCG Env V3. In contrast, neutralization was not observed against HIV-$1_{SF33/X4}$, which has a heterologous V3 sequence, nor was it found against primary HIV-1 R5 isolates from either clade A or B. Furthermore, the viral load in the vaccinated macaques was significantly reduced following low-dose challenge with SHIV-MN, and early plasma viremia was markedly decreased after high-dose SHIV-MN challenge. In contrast, replication of pathogenic SHIV-89.6PD was not affected by vaccination in any of the macaques. Thus, we have shown that immunization with an rBCG Env V3 vaccine elicits a strong, type-specific V3 NAb response in rhesus macaques. While this response was not sufficient to provide protection against a pathogenic SHIV challenge, it was able to significantly reduce the viral load in macaques following challenge with a nonpathogenic SHIV. These observations suggest that rBCG vectors have the potential to deliver an appropriate virus immunogen for desirable immune elicitations.

Development of a preventive vaccine against human immunodeficiency virus type 1 (HIV-1) is urgently needed to control the spread of the virus worldwide. Although the immunological parameters that correlate with protective immunity against natural infection with HIV-1 are not fully known, it is assumed that a preventive vaccine must elicit potent, broadly reactive immunity against divergent strains of HIV-1 (25, 36, 42). Several recent studies have demonstrated that induction of virus-specific T-cell responses can confer protective immunity in nonhuman primate models, and these responses may also play a role in controlling HIV-1 replication in humans (6, 18, 19, 31, 33, 34, 38, 45, 48). Vaccine constructs containing viral *env* genes, in addition to *gag* and *pol*, have been shown to effectively control replication of challenge viruses (2, 5, 10), suggesting that neutralizing antibody (NAb) responses might also contribute to protection against pathogenic infection or disease progression. Passive transfer of serum immunoglobulin from chimpanzees experimentally infected with several different HIV-1 isolates has been shown to block the establishment of a simian immunodeficiency virus (SIV)-HIV chimeric simian-human immunodeficiency virus (SHIV) infection in pig-tailed macaques (37, 46). It is not known, however, whether vaccines that actively elicit a potent NAb response can provide protection in nonhuman primates challenged with SHIV.

Previously, we demonstrated that recombinant *Mycobacterium bovis* bacillus Calmette-Guérin (rBCG), which secretes a chimeric protein consisting of the V3-neutralizing epitope of HIV-1 and α-antigen (rBCG Env V3), can induce HIV-1-specific NAb in a small-animal model (9, 15, 16). BCG was selected as a vaccine vehicle because it has several characteristics that are considered efficacious for developing a candidate

* Corresponding author. Mailing address: AIDS Research Center, National Institute of Infectious Diseases, Shinjuku-ku, Tokyo 162-8640, Japan. Phone: 81-3-5285-1111, ext. 2737. Fax: 81-3-5285-1183. E-mail: someyan@nih.go.jp.

HIV-1 vaccine (1, 49), including the ability to induce long-lasting immune responses (7). It is generally accepted that a candidate vaccine against HIV-1 must also be easily administered and affordable in developing countries, and it must be compatible with other commonly administered vaccines (35). If effective, a BCG-based recombinant HIV-1 (rBCG–HIV-1) vaccine would fulfill many of these critical requirements.

Results using other vaccine modalities, in particular, live attenuated SIV vaccines, have raised concerns about the potential for reversion to pathogenicity (3, 4), suggesting that many SIV strains may be potentially virulent. In this study, we used two distinct strains of challenge virus: SHIV-MN (29), which contains V3 sequences homologous to rBCG Env V3, and SHIV-89.6PD (12, 20, 28, 41), which is heterologous in the V3 region and highly pathogenic. We examined whether vaccination with rBCG Env V3 could effectively elicit NAb responses in rhesus macaques and whether it might effectively induce protective immunity against challenge with either SHIV-MN or SHIV-89.6PD.

MATERIALS AND METHODS

Animals. The macaques (*Macaca mulatta*) used in this study originated from China and were purchased through Japan SLC Ltd., Shizuoka, Japan. The animals were maintained according to standard operating procedures established for the evaluation of human vaccines at the Tsukuba Primate Center, National Institute of Infectious Diseases, Tsukuba, Ibaragi, Japan. The study was conducted in the P3 facility for monkeys in the Murayama Branch, National Institute of Infectious Diseases, Musashimurayama, Tokyo, Japan, and in accordance with requirements specified in the laboratory biosafety manual of the World Health Organization.

Construction of the rBCG Env V3 immunogen. rBCG substrain Tokyo was produced by transfection of BCG-Tokyo 172 cells with plasmid pSO246 as described previously (21, 22, 30). The XhoI site of this plasmid was used to insert a mycobacterial codon-optimized DNA fragment encoding 19 amino acids of the Japanese HIV-1 V3 consensus sequence (NTRKSIHIGPGRAFYATGS), which has a neutralization sequence identical to that of HIV-1_{MN} (16, 23, 39, 52). The resulting rBCG vector was designated rBCG Env V3. By semiquantitation of a chimeric protein consisting of the V3 peptides and α-K protein (9), the concentration of the secreted protein was estimated to range from 1 to 3 μg/ml in the culture filtrate of rBCG Env V3 (data not shown).

Viruses. Viruses used in challenge experiments were kindly provided by Y. Lu, Harvard AIDS Institute, Cambridge, Mass. The SHIV-MN virus stock was prepared in concanavalin A-activated macaque peripheral blood mononuclear cells (PBMC) from normal animals, and the amount of virus was quantified by SIV p27 antigen enzyme-linked immunosorbent assay (ELISA) (Coulter Co., Hialeah, Fla.). The tissue culture infective dose (TCID) of the stock was measured on CEMx174 cells (AIDS Research and Reference Reagent Program, National Institutes of Health, Rockville, Md.). Stocks of HIV-1_{MN} and HIV-1_{IIIB} (AIDS Research and Reference Reagent Program) were prepared by propagating 100 50% TCID ($TCID_{50}$) of each virus in phytohemagglutinin-activated normal human PBMC, as described previously (17). The primary isolate, HIV-1_{MNp}, was kindly provided by J. Sullivan, University of Massachusetts Medical School, Worcester, Mass. All other viruses were obtained from the AIDS Research and Reference Reagent Program. Cell-free virus stocks were stored at −130°C until they were used.

V3-specific ELISA. HIV-1 V3 peptide-based ELISAs were used for titration and quantification of serum antibodies for detection as described previously (14). In brief, 96-well ELISA plates (MaxiSorp; Nunc A/S, Roskilde, Denmark) were coated with 100 μl of peptide MN (DKRIHIGPGRAFYTT)/well in 50 mM carbonate buffer (pH 9.3) at 5 μg/ml overnight at 4°C. The wells were washed and treated with 5% nonfat milk in phosphate-buffered saline for 1 h at 37°C. Duplicate samples containing either control or test macaque serum at appropriate dilutions were then added at 100 μl/well, and the plates were incubated for 1 h at 37°C. The wells were washed and incubated with a detection antibody solution consisting of peroxidase-conjugated goat anti-monkey immunoglobulin G (IgG) antibody (EY laboratories Inc., San Mateo, Calif.) at 100 μl/well for 1 h at 37°C. After final washes with 0.05% Tween-20–phosphate-buffered saline (PBST), peroxidase substrate was added, and the reaction was stopped by the addition of 0.5 M H_2SO_4.

IFN-γ ELISPOT assay. Enzyme-linked immunospot (ELISPOT) assays were performed using the method developed by Mothe and Watkins of the Wisconsin University Primate Center and described elsewhere (18, 33). In brief, 96-well flat-bottom plates (U-CyTech-BV, Utrecht, The Netherlands) were coated with anti-gamma interferon (IFN-γ) monoclonal antibody before being washed with PBST and blocked with bovine serum albumin. Freshly isolated PBMC were mixed with either concanavalin A or 2 μM V3 peptide and were then incubated for 16 h at 37°C in 5% CO_2 in anti-IFN-γ-coated plates. Once the plates had been washed, rabbit anti-IFN-γ polyclonal biotinylated detector antibodies were added, and the plates were incubated. Gold-labeled anti-biotin IgG solution (U-CyTech-BV) was added to the plates after they were washed with PBST. The plates were then incubated for 1 h at 37°C. Developed wells were imaged, and spot-forming cells (SFC) were counted using the KS ELISPOT compact system (Carl Zeiss, Oberkochen, Germany). An SFC was defined as a large black spot with a fuzzy border (33).

In vitro virus neutralization assays. GHOST cell neutralization assays were performed as previously described (8). Briefly, GHOST cells expressing either CXCR4 or CCR5 were used as targets for HIV-1 infection (50, 54). The cells were analyzed by FACSCalibur flow cytometry (Becton Dickinson, San Jose, Calif.), and 15,000 events were scored. The mean number of fluorescent GHOST cells determined from negative controls plus 2 standard deviations was considered the cutoff for a positive sample. Purified human immunoglobulin (Nihon Pharmaceutical Co., Tokyo, Japan) and saline were included as additional controls.

M8166 cell-based virus neutralization assays were also performed as described previously (16, 47). In brief, the in vitro neutralization activity of purified macaque IgG was determined using 100 $TCID_{50}$ of either HIV-1_{MN} or SHIV-MN in cultures of M8166 cells. The results were compared with parallel cultures to which preimmune serum IgG was added. Neutralization was expressed as percent inhibition of HIV-1 p24 or SIV p27 antigen production in the culture supernatants. Purified normal macaque IgG was used as a control.

Quantification of cell-associated viral load. Levels of cell-associated virus were quantified by limiting dilution of PBMC (from 10^6 to 1 cells), and the virus was cocultured with M8166 cells as described previously (17). Virus released into the culture supernatant was measured by SIV p27 antigen ELISA (Coulter). The smallest number of PBMC required to produce a positive culture was considered the end point, and the titer of infectious virus was expressed as $TCID_{50}$ per 10^6 PBMC.

PCR detection of proviral HIV-1 infection of rhesus macaques. PBMC with SHIV were detected by DNA PCR using a primer pair that spans the C2-V3 sequence of HIV-1_{IIIB}, followed by Southern blotting with an SE1 probe, 5′-GCAGAAGAAGAGGTAGTAATTAGAT-3′ (nucleotides 7019 to 7043) (47). The positions of the oligonucleotides are numbered relative to the HIV-1_{HXB2} isolate in the ENTREZ database (National Center for Biotechnology Information, National Library of Medicine, National Institutes of Health, Bethesda, Md.). Viral DNA was quantified by comparison with standards derived from 8E5/LAV cells, which contain one copy of HIV-1 proviral DNA per cell (AIDS Research and Reference Reagent Program).

Competitive PCR quantitation of SHIV RNA in plasma. Quantitative, competitive reverse transcription-PCR was performed using a competitor RNA and a DNA template as previously described (18, 32, 44). The detection limit of this assay was 500 RNA copies/ml in monkey plasma (18, 32).

Sequencing of HIV-1 Env C2-V3 sequence. To determine the sequence of the HIV-1 Env C2-V3 region, mRNA was extracted from stock virus and cDNA was synthesized using a Micro-FastTrack version 2.0 kit (Invitrogen, Carlsbad, Calif.) and a cDNA cycle kit (Invitrogen) according to the manufacturer's instructions. The PCR products were cloned into a pCR II vector with a dual promoter using a TA cloning kit (Invitrogen) (47). Sequence analysis was performed using a Big Dye terminator cycle-sequencing FS kit (Perkin-Elmer, Foster City, Calif.) and automated ABI 310 sequencer (Perkin-Elmer) with Sp6 and T7 sequence primers (Invitrogen). Sequence data were compared with published HIV-1 sequences in GenBank (National Center for Biotechnology Information, National Institutes of Health).

Statistical analysis. Calculations of the geometric mean ± standard deviation (SD) were carried out with a microcomputer. Significance was defined as a P value of <0.05.

RESULTS

Vaccination protocol. Twenty-four male rhesus macaques (R-01 through R-24) were enrolled in the study. Of these, 15 were subcutaneously immunized for 24 weeks with 10 mg of

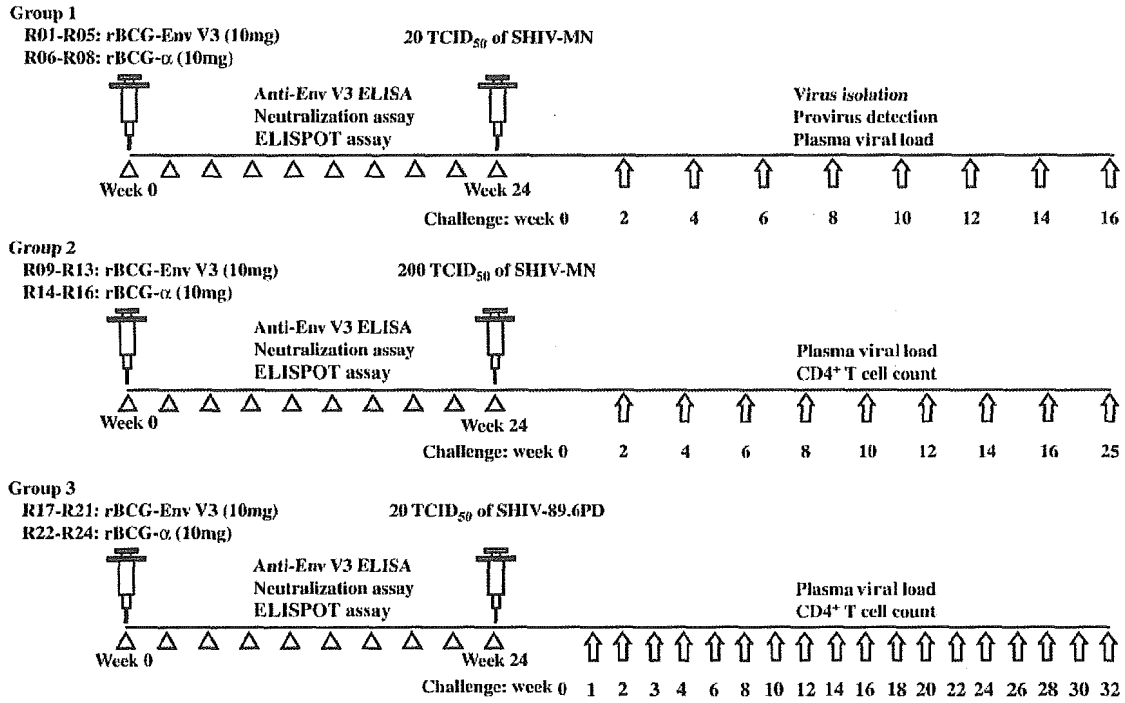

FIG. 1. Schematic representation of the experimental protocol for immunization of rhesus macaques with rBCG Env V3 and challenge with either SHIV-MN or SHIV-89.6PD. A total of 24 macaques were assigned to either the rBCG Env V3 vaccine or rBCG vector control group. The animals each received a single subcutaneous injection and were then split into three groups prior to challenge with either low-dose SHIV-MN, high-dose SHIV-MN, or SHIV-98.6PD.

rBCG Env V3 (16), which expresses and secretes a chimeric protein consisting of α-antigen and the Env V3 region of HIV-1_{MN}. The remaining nine macaques were immunized by the same route and with the same dose of rBCG α-antigen and served as vector controls. All macaques inoculated with rBCG Env V3 remained in good health following vaccination. Three of the 15 immunized macaques experienced transient redness with slight erosion localized at the injection site; however, the reaction spontaneously resolved within 3 months. Following immunization, the 24 macaques were divided into three groups, each group consisting of five immunized animals and three vector controls. The macaques within each group received an intravenous challenge with either SHIV-MN (20 or 200 $TCID_{50}$) or SHIV-89.6PD (20 $TCID_{50}$) (Fig. 1).

Vaccine-induced HIV-specific immune responses following rBCG Env V3 immunization. (i) Neutralizing antibodies. As described above, 15 rhesus macaques were vaccinated with a single subcutaneous inoculation of 10 mg of rBCG Env V3. Induction of HIV-1-specific immunity was measured 24 weeks later in blood samples obtained pre- and postvaccination. All 15 immunized macaques exhibited HIV-1 Env V3 peptide-binding antibody activity by ELISA at serum dilutions ranging from 1:640 to 1:10,240 (Fig. 2). Antibody responses were monophasic, peaking at 4 to 6 weeks and then gradually declining. Serum samples obtained from naïve macaques were consistently negative by ELISA, while postvaccination sera did not react with a control fusion peptide of HIV gp41 (data not shown).

Antibodies were purified from the macaque sera to remove factors that might interfere with certain bioassays (51). The purified antibodies were then tested in vitro for the ability to neutralize SHIV-MN infection in M1866 cells (Fig. 3). Antibodies induced in macaques vaccinated with rBCG Env V3 strongly neutralized both the challenge SHIV-MN (grown in rhesus PBMC) and a T-cell line-adapted (TCLA) laboratory strain, HIV-1_{MN}. A mean 50% inhibitory concentration (IC_{50}) of 0.05 to 0.5 μg of IgG/ml was measured against SHIV-MN, and a mean IC_{90} of ~3.0 μg of IgG/ml was observed against HIV-1_{MN}. Neutralizing activity was detected in serum samples obtained 4 to 6 weeks after vaccination and was maintained for at least 24 weeks. Preimmune serum IgG from nine macaques immunized with vector alone, and IgG from three additional naive macaques (data not shown), did not neutralize either virus.

(ii) Neutralization responses against primary HIV-1 isolates. To further assess the specificity of antibodies in immune sera, neutralizing activity was evaluated against a panel of seven primary HIV-1 isolates using GHOST cells expressing either CCR5 or CXCR4 (Table 1). Purified IgG from macaques in each of the three immunization groups was able to effectively neutralize HIV-$1_{BZ167/X4}$, HIV-$1_{SF2/X4}$, and HIV-$1_{CI2/X4}$ (Table 1 and Fig. 4), with mean IC_{50} values of 5 to 7, 4 to 7, and 5 to 15 μg/ml, respectively. By comparison, neutralization of HIV-$1_{MNp/X4}$ required ~10-fold more serum IgG, with a mean IC_{50} of 50 μg/ml. Three additional isolates, HIV-$1_{SF33/X4}$, HIV-$1_{SF33/R5}$, and the clade A isolate HIV-$1_{VI313/R5}$,

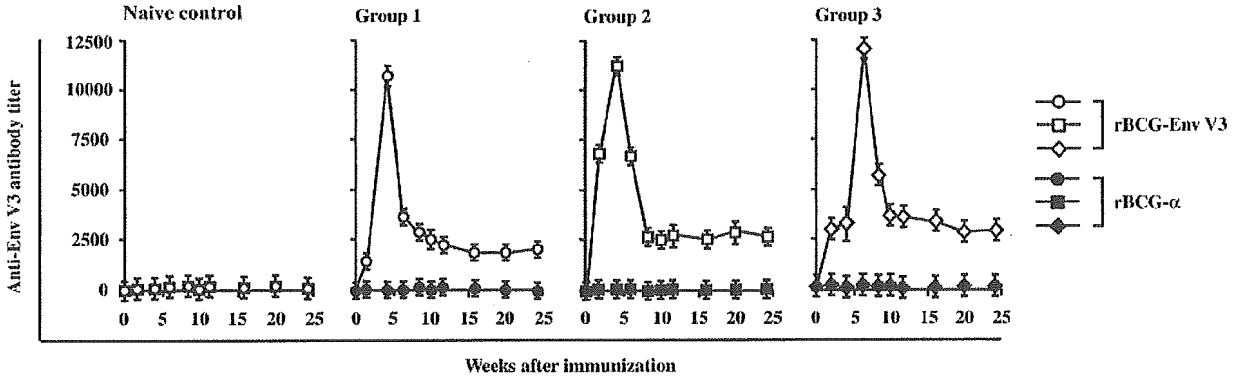

FIG. 2. Serum anti-V3 antibody titers determined by peptide-based ELISA. Preimmune and immune sera from macaques inoculated with rBCG Env V3 were collected and stored at −80°C until they were used. Sera from naïve macaques were used as controls. Data using preimmune sera were within the control levels (data not shown). The results are expressed as the means ± SD of four independent assays.

were not neutralized with serum IgG concentrations up to 50 μg/ml (Table 1). Preimmune sera had no neutralizing activity against any of the isolates. Thus, antibodies present in sera from the immunized macaques were able to neutralize primary HIV-1 isolates, including HIV-1_{BZ167}, HIV-1_{SF2}, and HIV-1_{CI2}, in assays using GHOST cells that express CXCR4 with 10- to 50-fold-higher sensitivity than that of the dual-tropic (X4-R5) TCLA strain HIV-1_{MNp}. Among the neutralization-sensitive viruses, the V3 sequence motifs of HIV-1_{BZ167} and HIV-1_{SF2} shown in Fig. 5 did not correlate with the observed neutralization profiles of HIV-1 Env V3.

(iii) V3 peptide-specific T-cell responses. Table 2 offers a comparison of the virus-specific T-cell response levels determined by IFN-γ ELISPOT analysis in immunized animals with the neutralization data provided in Fig. 2. Of the 15 animals immunized with rBCG Env V3 (180 and 160 SFC/10^6 PBMC at 6 weeks postimmunization [p.i.], respectively), only R-09 and R-10 showed very low levels of SFC activities at the time of

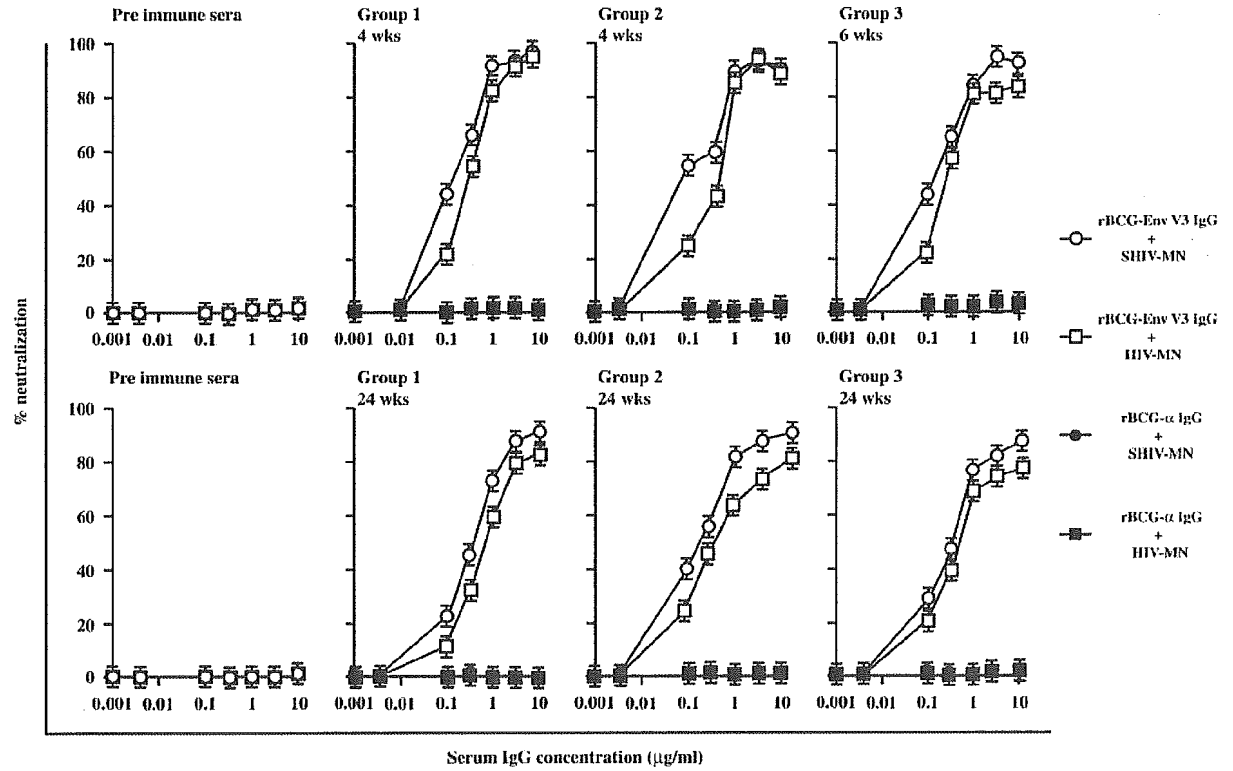

FIG. 3. HIV-1-specific neutralization antibody responses in macaques vaccinated with rBCG Env V3. Analysis of in vitro neutralization of SHIV-MN by anti-rBCG-HIV-1 antibodies using M8166 cell-based virus neutralization assays. Serum IgG was purified from preimmune or immune sera of macaques inoculated with rBCG Env V3 at the indicated times. The results are expressed as the means ± SD of four independent assays.

TABLE 1. 50% neutralization calculated on the basis of neutralization curves[a]

Serum sample	Neutralizing activity (μg)						
	BZ167/X4	MNp/X4	SF2/X4	SF33/X4	SF33/R5	V1313/R5	C12/X4
Group 1	6.5	50	7	>50	>50	>50	10
Group 2	5	50	4	>50	>50	>50	5
Group 3	7	50	6.5	>50	>50	>50	15
Pre immunization sera of groups 1, 2, and 3	>50	>50	>50	>50	>50	>50	>50

[a] The neutralization assays with the various viruses were carried out in GHOST cells expressing either CXCR4 (X4) or CCR5 (R5) as indicated in Fig. 4. BZ167, MNp, SF2, SF33, and CI-2 are HIV-1 clade B viruses. VI313 is an HIV-1 clade A virus.

SHIV challenge (120 and 110 SFC/10^6 PBMC at 24 weeks p.i., respectively) (Table 2). In contrast, <100 SFC/10^6 PBMC were observed in other immunized animals, and <20 SFC/10^6 PBMC were observed in controls. Thus, the V3 region antigen in the rBCG Env V3 proved unable to induce significant levels of virus-specific T-cell responses in immunized animals.

Challenge with low-dose SHIV-MN. The first group of eight macaques (R-01 through R-08), consisting of five animals that received rBCG Env V3 and three that received control rBCG α-antigen, were intravenously challenged with low-dose SHIV-MN (20 $TCID_{50}$) at 24 weeks p.i. The cell-associated virus load was measured in PBMC cocultures, and proviral copy numbers were estimated by DNA PCR using primary PBMC genomic DNA. The level of plasma viremia in each macaque was quantified by competitive reverse transcription-PCR to assess infection and virus replication for 16 weeks after virus challenge (Table 3).

Control macaques vaccinated with the vector alone (R-06 through R-08) were positive in all three viral-load assays 2 weeks after SHIV-MN challenge and remained positive for a follow-up period of 10 weeks. Because only low levels of viral RNA (<10^4 RNA copies/ml) were transiently detected 2 weeks postchallenge, all three assays (virus isolation, plasma RNA, and proviral DNA) were used for virus detection. Using these criteria, we observed that all three parameters remained negative after low-dose SHIV-MN challenge in three of five macaques vaccinated with rBCG Env V3 (R-02, R-04, and R-05). However, macaque R-01 was transiently positive in all three assays for virus infection at 4 weeks. Another macaque immunized with rBCG Env V3 (R-03) exhibited a sharp in-

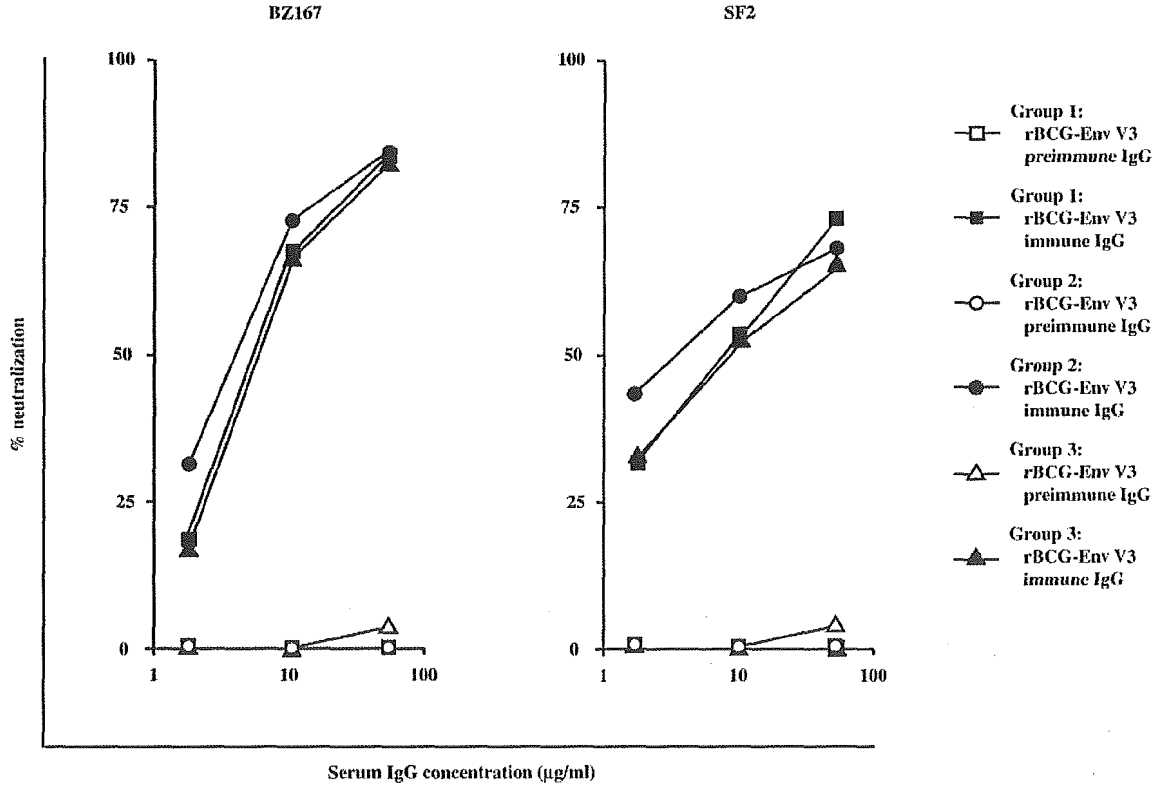

FIG. 4. Neutralization of HIV-1_{BZ167} and HIV-1_{SF2} in GHOST-X4 cells by immune sera from macaques vaccinated with rBCG Env V3. Dilutions of immune sera (closed symbols) and preimmune sera (open symbols) were tested in duplicate, and the percent neutralization was calculated using the mean value. The dose-response curves represent the means of three independent assays.